AD-A039 605 WATERVLIET ARSENAL N Y F/G 19/6
ULTRASONIC AND ACOUSTIC HOLOGRAPHIC TECHNIQUES FOR INSPECTION O--ETC(U)
MAR 77 G P CAPSIMALIS, G D'ANDREA

UNCLASSIFIED WVT-TR-77019 NL

1 OF 1
ADA039605

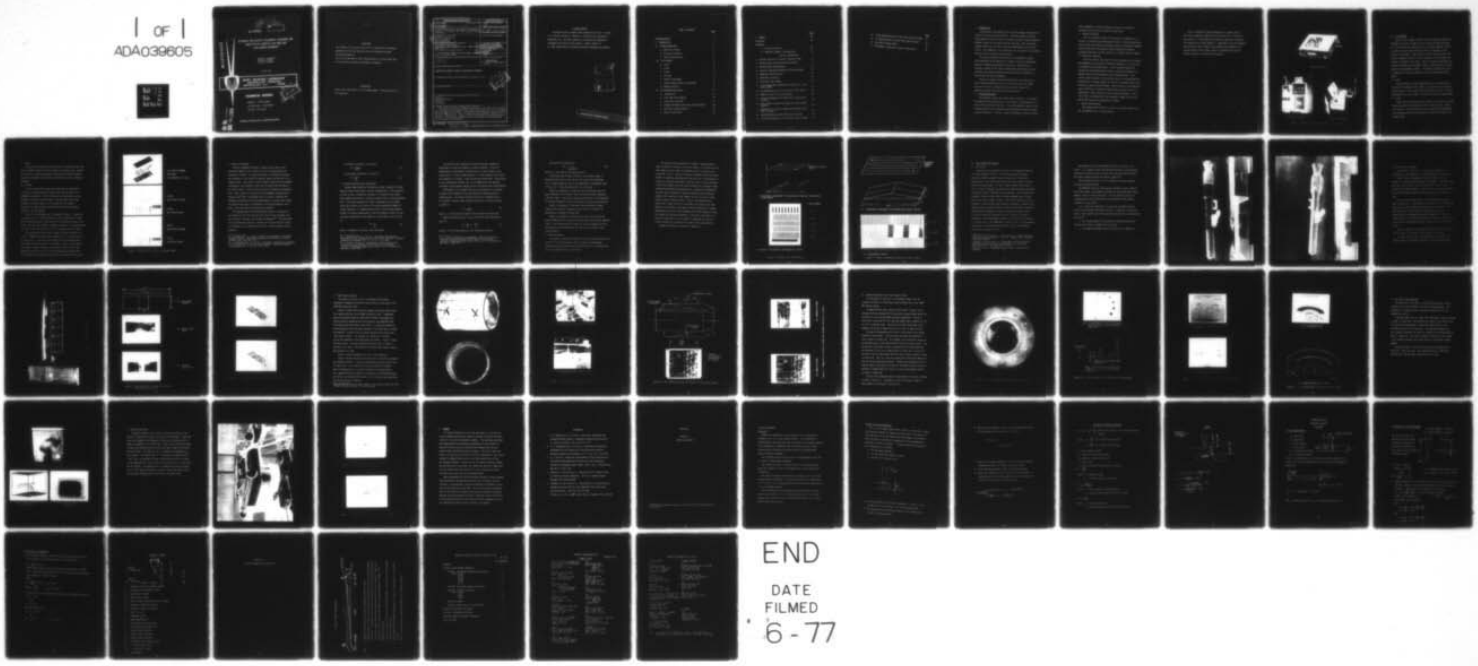

END

DATE FILMED
6-77

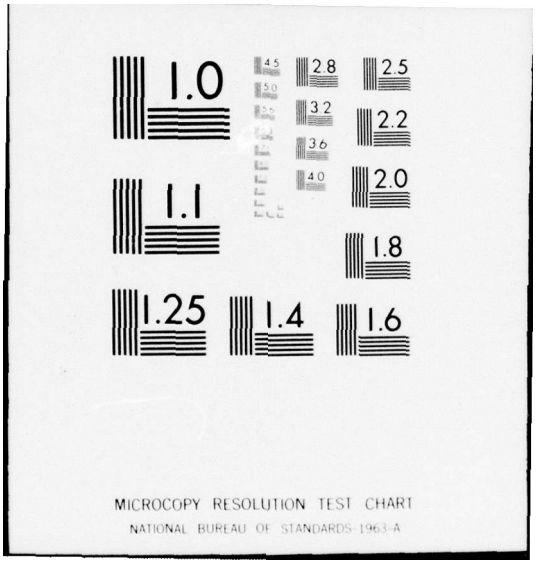
1.0
1.1
1.25
1.4
1.6
1.8
2.0
2.2
2.5
2.8
3.2
3.6
4.0
4.5
5.0
MICROCOPY RESOLUTION TEST CHART
NATIONAL BUREAU OF STANDARDS-1963-A

WVT-TR-77019

ULTRASONIC AND ACOUSTIC HOLOGRAPHIC TECHNIQUES FOR INSPECTION OF COMPOSITE GUN TUBES AND OTHER WEAPON COMPONENTS

George P. Capsimalis
Giuliano D'Andrea
Ralph E. Peterson

March 1977

BENET WEAPONS LABORATORY
WATERVLIET ARSENAL
WATERVLIET, N.Y. 12189

TECHNICAL REPORT

AMCMS No. 611101.91A0011

DA Project No. 1T161101A91A

Pron No. M1-7-51701

DISCLAIMER

The findings in this report are not to be construed as an official Department of the Army position unless so designated by other authorized documents.

The use of trade name(s) and/or manufacturer(s) in this report does not constitute an official indorsement or approval.

DISPOSITION

Destroy this report when it is no longer needed. Do not return it to the originator.

SECURITY CLASSIFICATION OF THIS PAGE (When Data Entered)

REPORT DOCUMENTATION PAGE

READ INSTRUCTIONS BEFORE COMPLETING FORM

1. REPORT NUMBER: WVT-TR-77019	2. GOVT ACCESSION NO.
3. RECIPIENT'S CATALOG NUMBER	
4. TITLE (and Subtitle): Ultrasonic and Acoustic Holographic Techniques for Inspection of Composite Gun Tubes and Other Weapon Components.	5. TYPE OF REPORT & PERIOD COVERED: Technical rept.
	6. PERFORMING ORG. REPORT NUMBER
7. AUTHOR(s): George P. Capsimalis, Giuliano D'Andrea, Ralph E. Peterson	8. CONTRACT OR GRANT NUMBER(s)
9. PERFORMING ORGANIZATION NAME AND ADDRESS: Benet Weapons Laboratory, Watervliet Arsenal, Watervliet, N.Y. 12189, SARWV-RT-TP	10. PROGRAM ELEMENT, PROJECT, TASK AREA & WORK UNIT NUMBERS: AMCMS No. 611101.91A0011, DA Proj. No. 1T161101A91A, Pron No. M1-7-51701
11. CONTROLLING OFFICE NAME AND ADDRESS: US Army Armament Research and Development Command, Dover, New Jersey 07801	12. REPORT DATE: March 1977
	13. NUMBER OF PAGES: 58
14. MONITORING AGENCY NAME & ADDRESS (if different from Controlling Office): 59 p.	15. SECURITY CLASS. (of this report): UNCLASSIFIED
	15a. DECLASSIFICATION/DOWNGRADING SCHEDULE

16. DISTRIBUTION STATEMENT (of this Report)

Approved for public release; distribution unlimited.

17. DISTRIBUTION STATEMENT (of the abstract entered in Block 20, if different from Report)

18. SUPPLEMENTARY NOTES

19. KEY WORDS (Continue on reverse side if necessary and identify by block number)

Acoustics
Composite Materials
Holography
Ultrasonics

20. ABSTRACT (Continue on reverse side if necessary and identify by block number)

Ultrasonic and acoustic holographic imaging has been shown to be an effective procedure for the nondestructive inspection of flaws and voids in composite and other material structures. Techniques for quantitatively imaging the size, shape and distribution of flaws in composites and conventional materials are discussed. Additionally a number of test results representing applications of ultrasonic and holographic imaging and their adaptation to typical material testing problems are presented.

DD FORM 1 JAN 73 1473 EDITION OF 1 NOV 65 IS OBSOLETE

371 050

SECURITY CLASSIFICATION OF THIS PAGE (When Data Entered)

ACKNOWLEDGEMENTS

The authors wish to express their appreciation to Drs. V. Nealy, H. D. Collins, and Mrs. N. Knutter, P. Gribble and R. Robinson of Holosonics Inc., for their technical instruction and cooperation throughout the course of this project. Special thanks to Mr. Paul Croteau for his valuable assistance throughout the program.

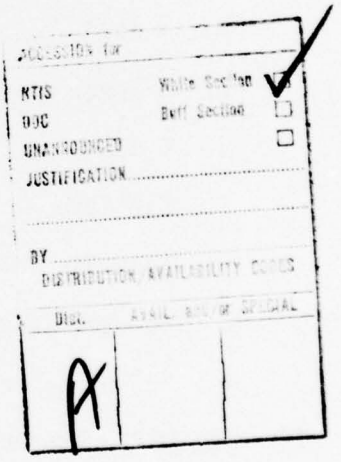

TABLE OF CONTENTS

LIST OF ILLUSTRATIONS

I. INTRODUCTION

High strength, high modulus and low density weapon components are essential for many Army applications. Composite materials provide these properties and are used in gun tubes and other related components. However, because of the nature of these materials, they can develop internal flaws such as voids, cracks and delaminations during fabrication. Such anomalies, if not detected, can contribute to catastrohpic failure as well as early fatigue failure.

This report describes an ultrasonic and holographic imaging system employed for the detection of defects which are inadverently present in manufactured composite structures. Additionally it provides a number of test results representing applications of the ultrasonic and acoustic imaging technique and their adaptation to typical material testing problems.

Finally the imaging technique developed for the detection of flaws provided quantitative results of the flaw sizes and shapes which are critical in assessing the structural integrity of a composite component for quality assurance purposes.

II. SYSTEM DESCRIPTION

The Holosonics' Model 200 system shown in Figure 1 is an Acoustic Holography imaging system which is also capable of performing A, B, C, and 3-D Scan ultrasonic functions. The system operates either in the through-transmission of pulse-echo mode and employs primarily ceramic focused transducers. The basic system configuration consist of three

major components; a digital mechanical scanner, an electronic processor and an optical (hologram) reconstructor.

A. Mechanical Scanner

This unit provides a means of traversing the transducer in a precise x-y scanning and stepping motion over a selected sample area. In this manner the scanning transducer creates a coordinate reference frame through which the detected signal (amplitude and phase) accurately describes the flaw position (x-y) within the test sample.

B. Electronic Processor

This unit receives the signal from the transducer on the scanner and depending on the settings selected a hologram, B, C or 3-D Scan is recorded on the storage scope. In the coherent holographic setting the time gated received signal is mixed and compared to a coherent phase shifted reference signal from the pulser. This mixing allows the phase of the received signal to be determined and registered on a storage scope as a function of transducer motion thus creating a complete phase hologram. Phase shifting of the reference signal simulates an inclined incident plane wave which serves to superimpose a linear grating on the constructed hologram. This in turn allows the separation of the holographic image from the zero order light during the reconstruction process.

C. Optical Reconstructor

The reconstructor consists of a laser, an optical bench with a lens arrangement and a TV video display.

After a hologram has been constructed on a storage scope, a hard copy recording is obtained on 46L Polaroid film. The film is then placed in a liquid gate of the optical system and illuminated with coherent laser light (6328 A°). Adjustment of the lens assembly then allows the focal plane of the hologram being examined to be scanned through various depth planes of information and resolve (focus) them one at a time on the TV monitor.

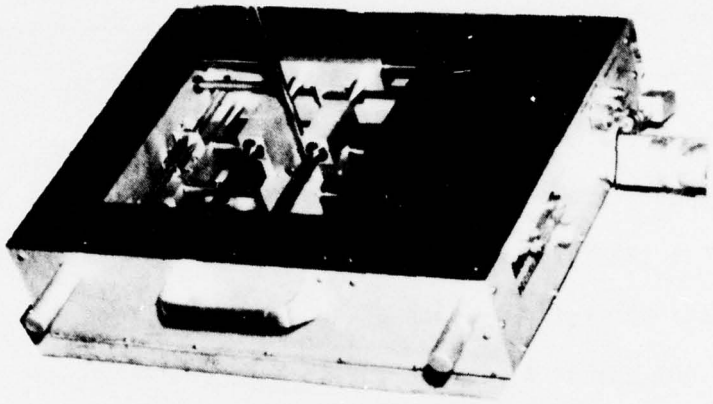

MECHANICAL SCANNER

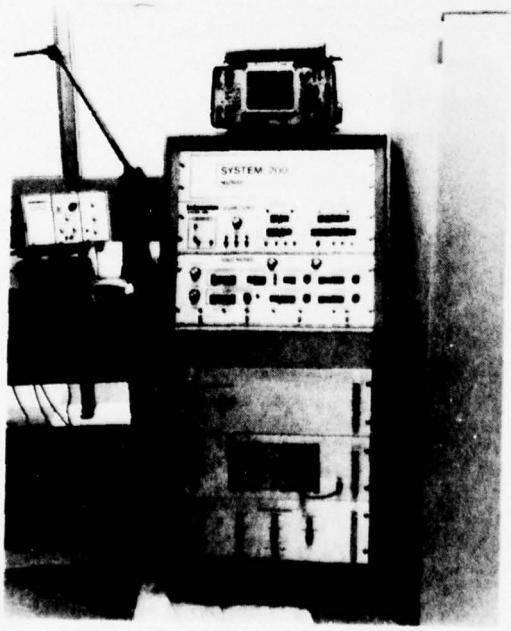

ELECTRONIC PROCESSOR

OPTICAL RECONSTRUCTOR

Figure 1. Scanned, acoustical, holographic imaging system.

III. TEST METHODS

Testing of the samples was done using the Holosonics Model 200. Although the system is capable of both contact and immersion modes all of the results were obtained with the samples immersed in water in order to transmit the sound waves from the transducer to the material being tested. High resolution results were obtained using ceramic transducers having 1" active diameter, 4" focal length and ranging in frequency from 1-5MHz. Both the through transmission and pulse-echo methods were employed in order to better depict the flaws present in the composite samples. The types of presentations used in imaging the flaws were obtained using the following operating modes:

A. A-Scan

A-Scan presents an oscilloscope display of the amplitude and distance of the detected flaw signal as a function of time from the transmit pulse. This initial search identifies the flaw, its depth, approximate size and is useful in setting up the other imaging modes.

B. B-Scan

B-Scan uses the processed A-Scan signals to display on a storage scope the depth and distribution of flaws present within a sample cross section. A precalibration allows accurate depth measurements to be obtained directly from the stored display on the face of the storage scope.

C. C-Scan

C-Scan uses the processed A-Scan signals to provide a plane view of the internal flaws of the test sample on a storage scope. Because this mode is an amplitude detection technique the system parameters should be calibrated for the desired sensitivity on known resolution standards.

D. 3-D Scan

In the 3-D Scan, the C-Scan and B-Scan data are processed to display on a storage scope the image of the flaws by means of an axomometric projection. The 3-D image may be projected at any pre-selected tilt and/or rotation angle. Also the front and/or back surfaces of the test object may be included in the isometric projection in order to more clearly depict the flaw distribution present in the test object.

The B, C, and 3-D modes are illustrated in Figure 2. Shown are the results of a 0.5" thick aluminum test block machined with three sets of flat bottom drill holes placed into the bottom surface of the block. The first set of holes is spaced to display a 3-D configuration. The holes in the 3-D set are all 0.125" in diameter and 0.25" deep.

The second set of holes forms a column in which the holes are 0.125" in diameter and ascend from a depth of 0.1" to a depth of 0.4" in steps of 0.1". The third set provides the same ascending order except that the holes are 0.25" in diameter. The B, C, and 3-D outputs shown in Figure 2 provide a multiview of the test block that completely describes the drill hole configuration and demonstrates the versatility and resolution available in examining thin structures.

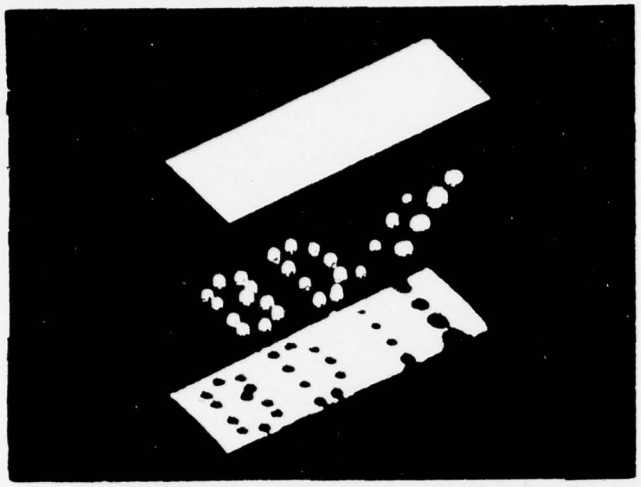

3-D VIEW OF STANDARD

TEST BLOCK

(45° ROTATION, 15° TILT)

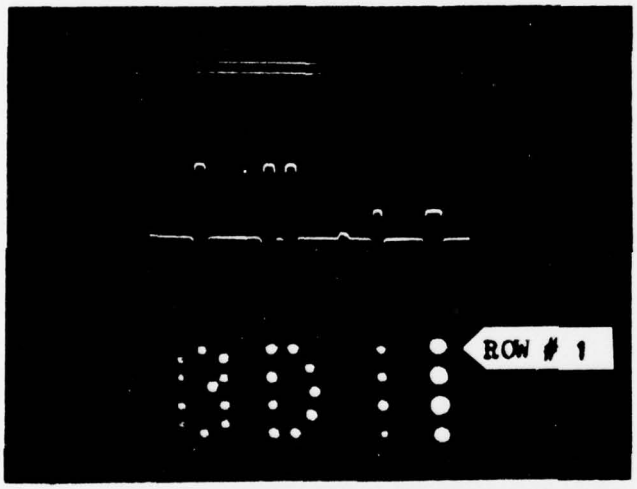

B-SCAN

SIDE VIEW OF 1ST ROW

C-SCAN

PLAN VIEW OF BLOCK

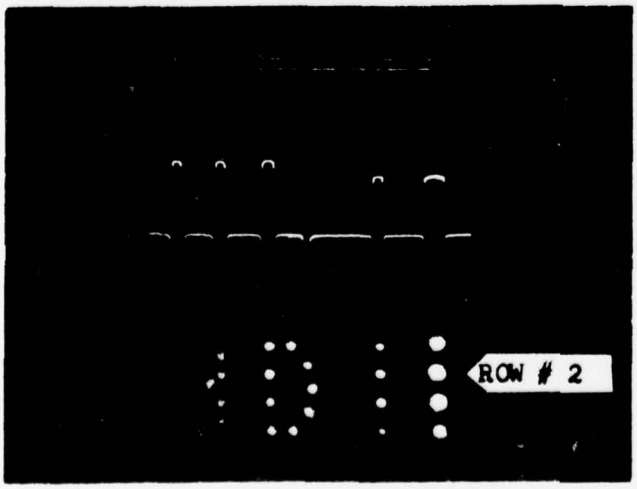

B-SCAN

SIDE VIEW OF 2ND ROW

C-SCAN

PLAN VIEW OF BLOCK

Figure 2. Imaging views of various ultrasonic modes.

E. Acoustic Holography

Acoustic Holography describes a method used to obtain high resolution imaging of the interior of thick structures which are transparent to sound. An acoustic hologram is obtained by focusing the transducer at the surface of the test sample and driving it by a coherent pulse. The sample is then diffusely insonified with coherent ultrasound as the transducer scans over the sample and the phase of the return signal is used to form the acoustic hologram on transparent film. Then by means of an optical lens arrangement (reconstructor) coherent light from a helium-neon laser is used to illuminate the hologram and project the reconstructed image on a ground glass screen. The reconstructed image is displayed on a television monitor, from which a hard copy Polaroid picture may be obtained.

The magnification of the reconstructed image is a function of the distance of the flaw from the focal plane of the transducer and the ultrasonic frequency used to make the hologram[1,2]. The resolution of the reconstructed image is a function of the wave length of sound in the medium λs, the distance to the flaw r and the aperture of the hologram L.

---

[1]B. B. Brenden and H. D. Collins, "Acoustical Holography with Scanned Hologram Systems", Holographic Nondestructive Testing, pp. 405-428 Academic Press, New York, 1974.

[2]B. P. Hildebrand and H. D. Collins, "Evaluation of Acoustical Holography for the Inspection of Pressure Vessel Sections", Materials Research and Standards, Vol. 12, No. 12, p. 23, 1972.

The lateral resolution is given by[2]:

$$\Delta x = \frac{1.22\lambda sr}{2L} \tag{1}$$

and the depth resolution is given by[2]:

$$\Delta\lambda = \frac{\lambda sr^2}{2L} \tag{2}$$

F. Focused Image Acoustical Holography[3]

Focused Image Acoustical Holography provides a method of contour mapping internal and external surface irregularities in thin materials. In order to map a surface the transducer is focused at the surface being imaged and driven by a coherent transmit pulse a few microseconds wide. Using phase detection an image is generated on the storage scope which consists of a series of fringes representing changes in surface elevation. As demonstrated by Collins the distance between fringes is directly proportional to the wave length of sound (λs) and inversely proportional to the number of signal echoes K and is given by:

$$\Delta Z = \frac{\lambda s}{2K} \tag{3}$$

where ΔZ represents the surface depth deviations.

---

[2]B. P. Hildebrand and H. D. Collins, "Evaluation of Acoustical Holography for the Inspection of Pressure Vessel Sections", Materials Research and Standards, Vol. 12, No. 12, p. 23, 1972.

[3]H. D. Collins, "Acoustical Interferometry Using Electronically Simulated Variable Reference and Multiple Path Techniques", Acoustical Holography, Newell Booth, Editor, Vol. 6, Plenum Press, New York, p. 597, 1975.

The multiple echo interference technique provides substantial improvement in resolving changes in surface elevation. Figure 3A demonstrates an experimental configuration of contour imaging a flat surface which is inclined approximately 1° to the reference plane where the transducer is scanned. Figure 3B provides experimental visualization of the interference relation (Eq 3) and demonstrates the improved resolution being attained through the use of multiple echo interferometry.

Additionally it was shown[3] that the fringe density is a function of phase shift frequency of the electronically simulated acoustic reference beam. The result of phase shifting the reference wave is to simulate a variable angle reference beam with a reference spacing d_x given by

$$d_x = \frac{\lambda s}{\sin \alpha_x} \tag{4}$$

where α_x is the inclination angle of the simulated reference wave.

When the reference wave is phase shifted the depth deviation is given by:

$$\Delta Z = \frac{\lambda s}{2K} \left(1 - \frac{\Delta X}{d_x}\right) \tag{5}$$

where ΔX is the fringe spacing on the interference pattern.

---

[3] H. D. Collins, "Acoustical Interferometry Using Electronically Simulated Variable Reference and Multiple Path Techniques", Acoustical Holography, Newell Booth, Editor, Vol. 6, Plenum Press, New York, p. 597, 1975.

Also Collins has shown that

$$\Delta X = \frac{\lambda s}{2Km_x + \lambda s/d_x} \qquad (6)$$

where m_x is the slope of the imaged surface.

The obvious use of phase shifting is to provide a means of determining the sign of the slope of the surface being examined. This is demonstrated by means of the experimental arrangement shown in Figure 4A. Figure 4B demonstrates the following:

Region Y_3 represents a fringe spacing which results from the phase difference of the return signal and the electronic simulated reference signal. The spacing though characteristic of the magnitude of the depth deviation ΔZ does not measure the sign of the deviation.

Region Y_1 represents a reference spacing obtained by phase shifting the electronic reference signal which is equivalent to simulating an inclined reference beam.

Region Y_2 represents a fringe spacing which results from the phase difference of the received signal and the phase shifted reference signal. The fringe spacing of region Y_2 satisfies equation (6) and characterizes both the magnitude and sign of the (surface) slope being examined.

G. Method Selection

The ability to accurately describe flaw size and shape within the interior of a solid structure using the present system depends primarily upon the proper selection and execution of the method which will best accomplish the test objectives.

The selection of one method over another is based primarily upon the material thickness of the test sample. The different ultrasonic modes are most useful for samples that are relatively thin (less than 1 inch). The use of focused transducers with the obvious benefit of improved resolution and sensitivity for flaw detection is limited to the plane described by the focal point of the transducer. As the flaw distance from this plane increases its ultrasonic image resolution and sensitivity deteriorates. Acoustical holography on the other hand is generally capable of producing high resolution images of the interior of test samples that are very thick (from several inches to several feet). Since in the reconstruction process one is able to focus at any depth, the resolution of this method is not limited to any specific plane or depth but is rather determined by the size of the hologram and the wave length of sound. For example the resolution obtained by acoustical holography of a flaw ten inches deep in a test sample is comparable to that of a C-Scan resolution at a depth 1/8 inch deep in the same material.

System Calibration is described in Appendix A.

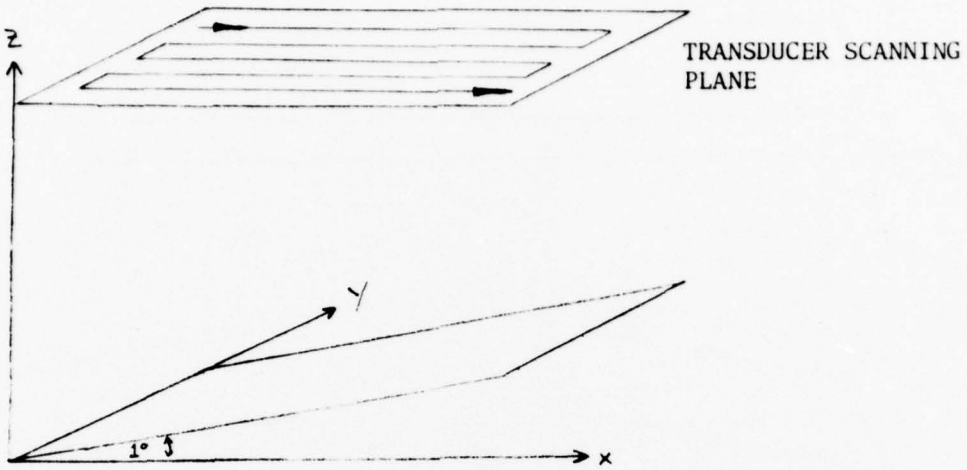

3A. EXPERIMENTAL ARRANGEMENT FOR DEMONSTRATING MULTIPLE ECHO ACOUSTIC INTERFEROMETRY

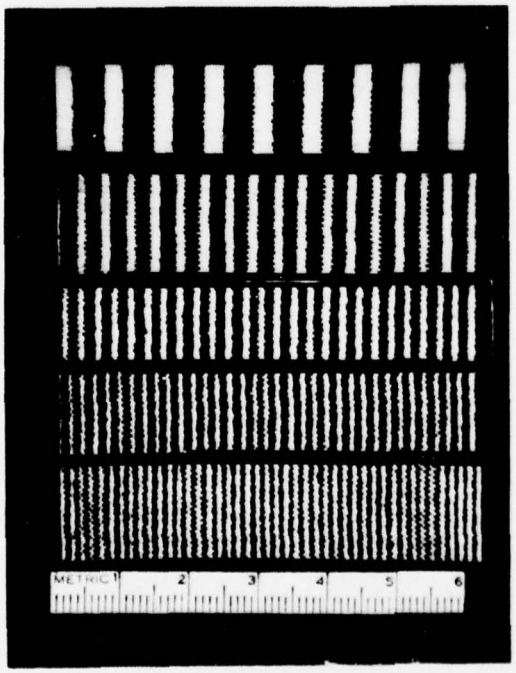

K (ECHO NUMBER)

K = 1

K = 2

K = 3

K = 4

K = 5

3B. MULTIPLE ECHO ACOUSTIC INTERFEROMETRIC RESULTS

Figure 3. Multiple echo interferometry.

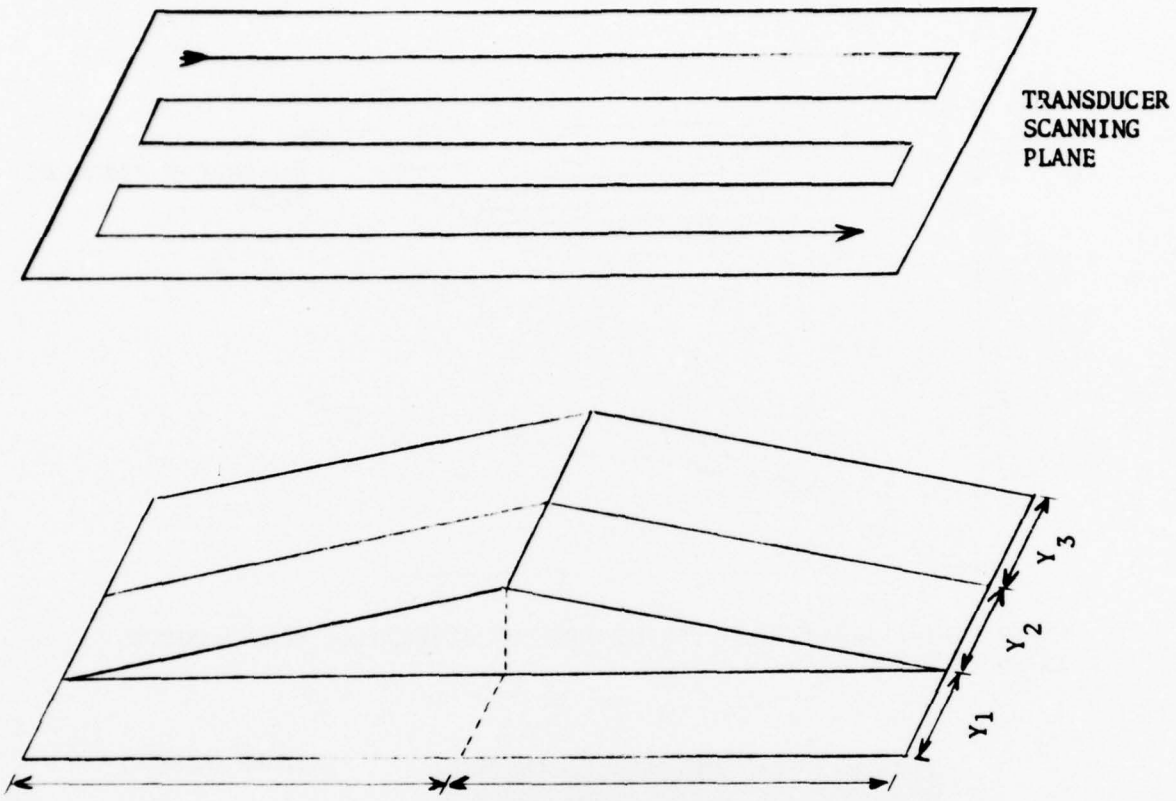

4A. EXPERIMENTAL ARRANGEMENT FOR DEMONSTRATING CONTOUR MAPPING

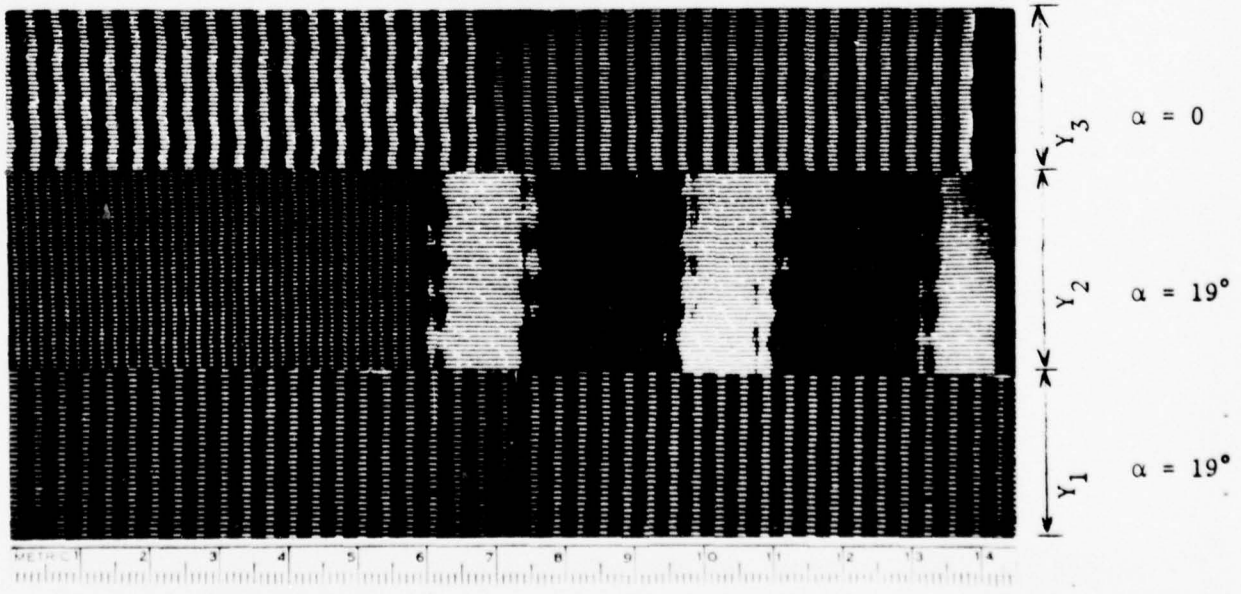

4B. INTERFEROMETRIC RESULTS

Figure 4. Acoustic interference mapping of planar surfaces.

IV. TEST PROBLEMS AND RESULTS

A. Introduction

Theoretical and experimental analyses of lightweight composite gun tubes commenced in 1964. At that time, Watervliet Arsenal started to establish general design criteria for a fiber glass wrapped steel liner which would satisfy pressure capability requirements and minimum weight. To date, several systems consisting of various liners, filaments and matrices have been designed, fabricated, and pressure tested. Materials used have been: steel (conventional, maraged), titanium alloys, glass filaments embedded into an epoxy matrix for liners; E-glass, S-glass, steel wire, graphite, boron for filaments; filled epoxies, epoxy novalac, polyimedes, aluminum alloy, magnesium alloy, titanium alloy for matrices (References 4 through 6). Considerable improvements in present lightweight weaponry can be achieved by supplying advancements made in composite materials technology. These improvements provide up to a 50% weight reduction in a system such as the 106MM M40A1 recoilless (Ref 4), and complete flexibility in disposable weapon concepts such as the 81MM XM73 Recoilless Gun Launcher (Ref 5).

---

[4] D'Andrea, G. and Cullinan, R., "Application of Filament Winding to Cannon and Cannon Components. Part III: Summary Report, November 1976, WVT-TR-76035.

[5] D'Andrea, G. and Cullinan, R., "Development of Design Analysis, Manufacturing and Testing of the 81MM XM73 Fiber Glass-Epoxy Recoilless Rifle", June 1974, WVT-TR-74014.

[6] D'Andrea, G. et al, "105MM M68 Thermal Shroud", November 1972, WVT-7249.

When weapons such as the 81MM XM73 RCLR, are released to the troops, it is imperative that they perform according to specifications. They must be tested in order to ensure that they meet the reliability and safety standard required of military components.

The following write-up is a first attempt to inspect composite gun tubes non-destructively.

The 81MM XM73 Reccilless Gun Launcher (Figures 5 and 6), made of Fiber Glass Epoxy, was designed, manufactured, and tested under hydrodynamic as well as firing pressures. The gun launcher consists of a forward barrel and an aft-nozzle joined together, after loading, by means of a scarf joint.

It is, then, very important to assure that the proper bonding exists in the chamber area before the RCLR is released. Preliminary work to check feasibility of the System 200 consisted of non-destructive testing of:

a. Two filament wound flat specimens, one bonded approximately 100% while the other is bonded only at the ends.

b. Two 81MM XM73 chamber sections as described in Appendix B.

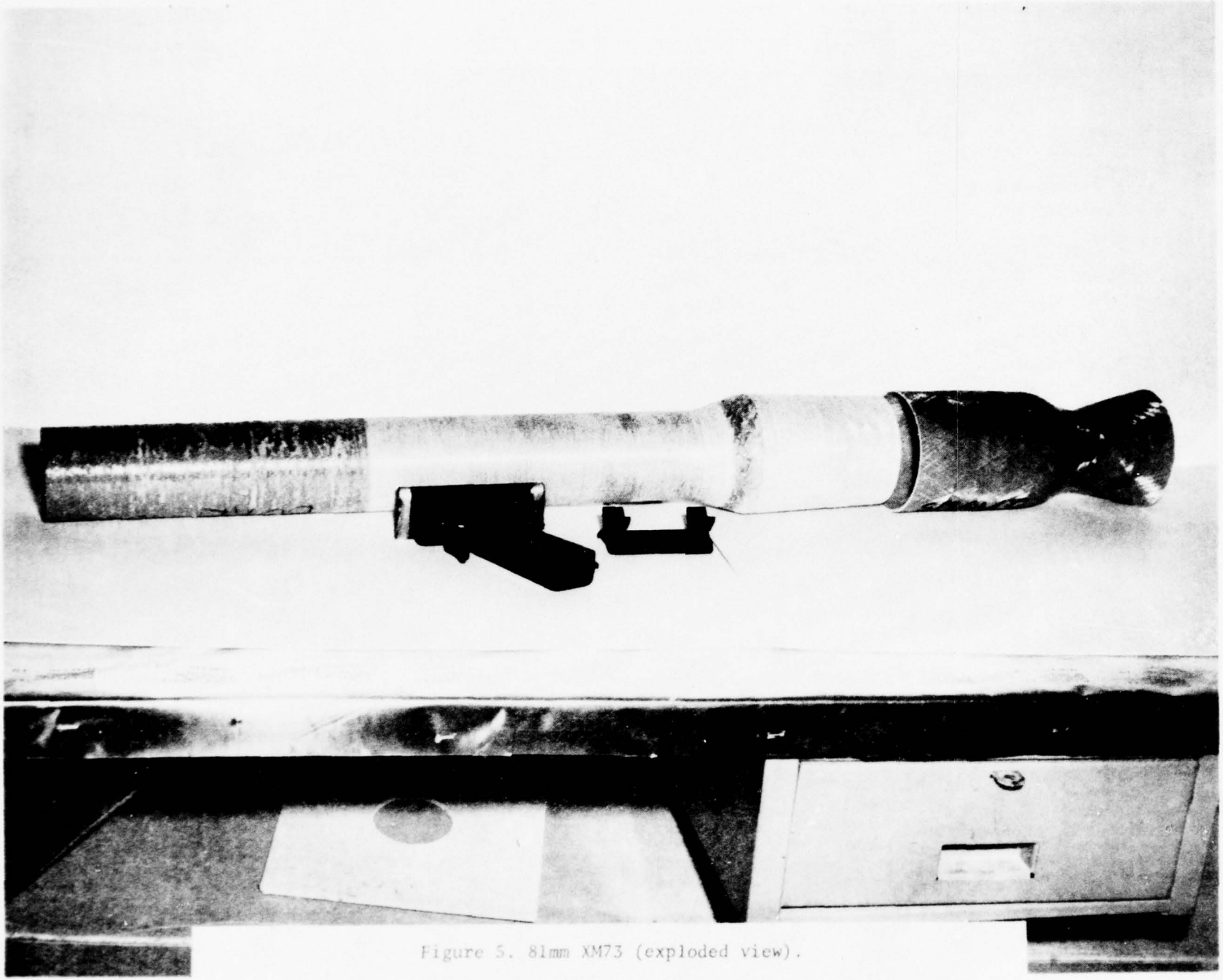

Figure 5. 81mm XM73 (exploded view).

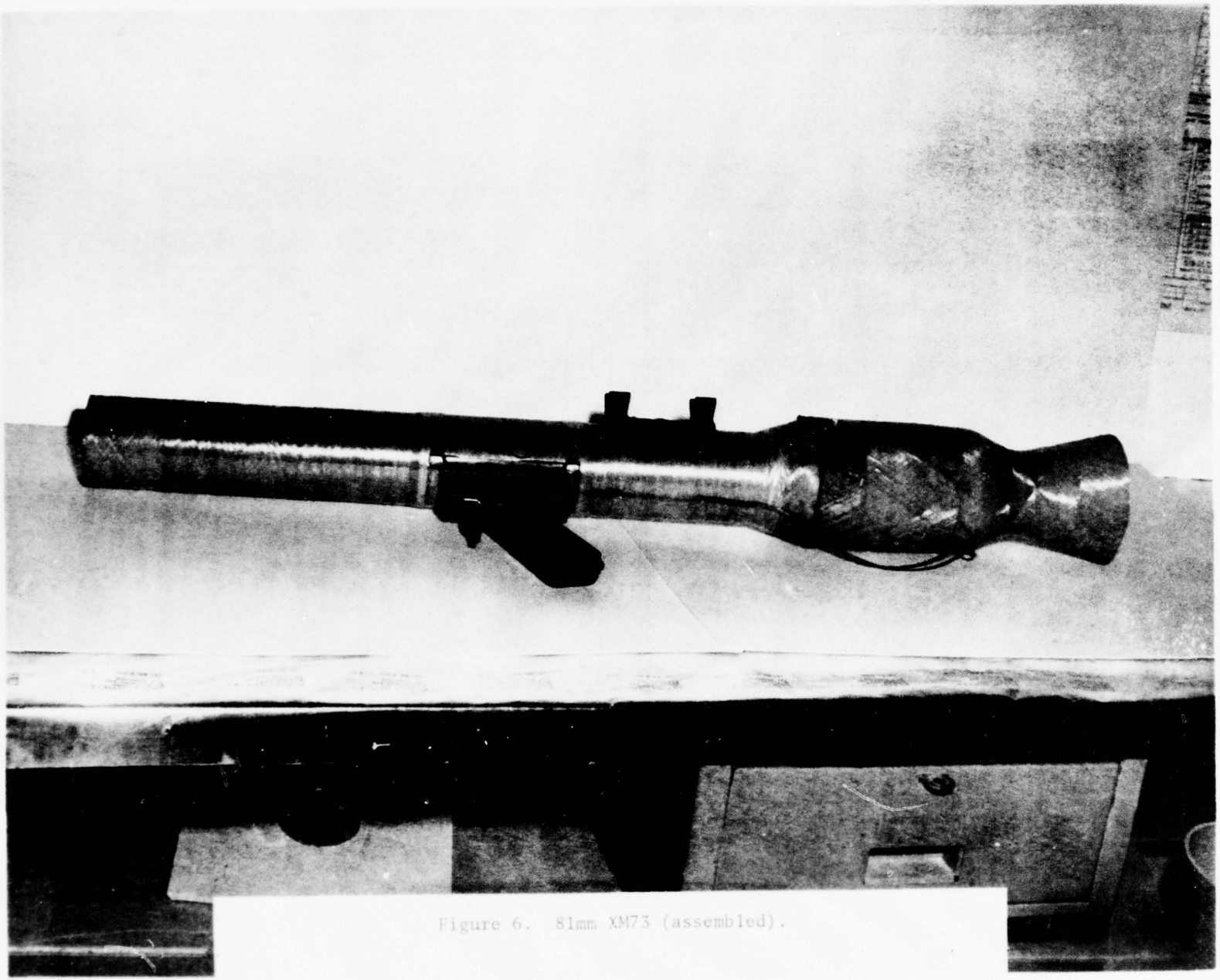

Figure 6. 81mm XM73 (assembled).

B. Flat Fiber Glass Samples

The objective of this test is to determine debonding and delamination at the interface of a composite/composite flat joint.

Figure 7 gives the geometry of the flat fiber glass test samples. One sample had the diagonal joint bonded. The other sample was glued on the perifery of the diagonal joint, thus leaving a disbond area of approximately 1" wide by 2" long. Since the samples were thin a through transmission technique was used for these two scans.

Figures 8B and 8C show C-Scans of the bonded and disbonded areas, respectively. The disbond area of the joint in the flat fiber glass piece is shown clearly by the dark area in Figure 8C. The other dark areas in both pictures represent flaws that were unintentionally introduced during sample preparation. Using the system magnification (which is approximately 0.45x) the dimensions of the flaw areas are obtained from the actual pictures of Figures 8B and 8C.

Figure 9 represents 3-D representation of the disbonded sample with the gate set to outline a thin layer of the material.

The above results clearly demonstrate the capability of the method to depict the disbond conditions of flat composite samples.

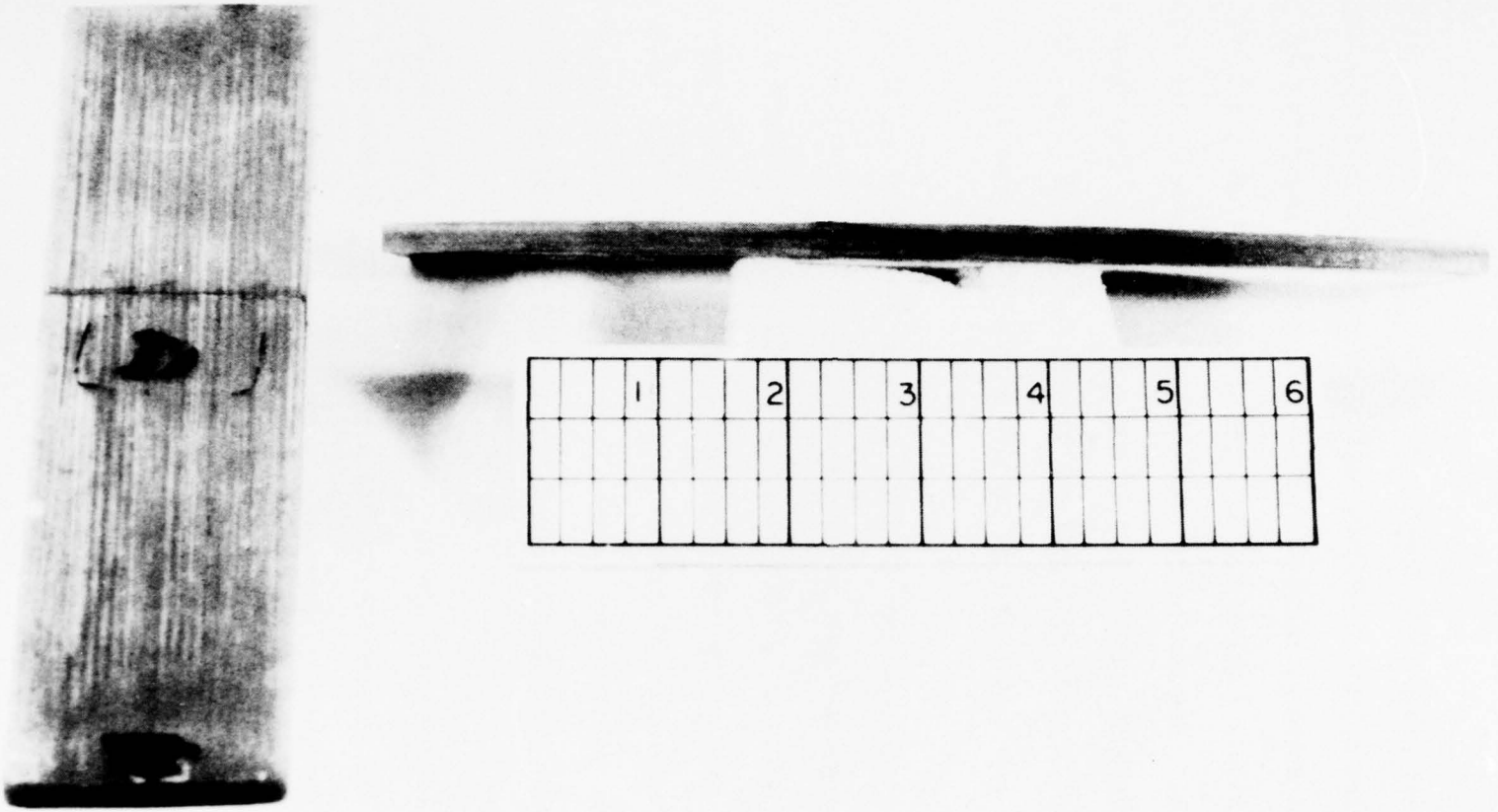

Figure 7. Flat fiber glass sample.

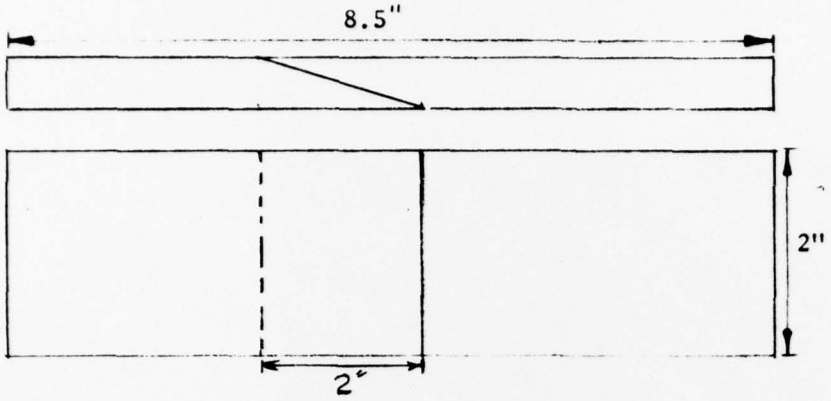

8A. FLAT SAMPLE GEOMETRY

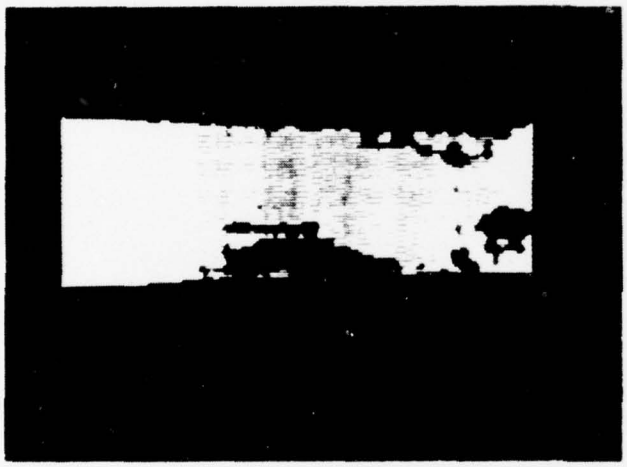

8B. BONDED CENTER JOINT

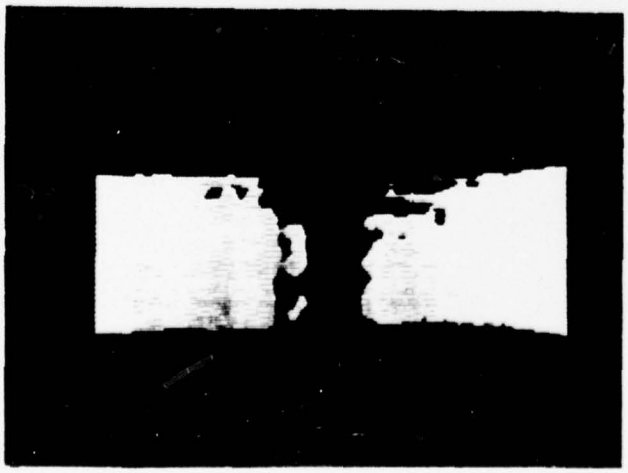

8C. UNBONDED CENTER JOINT

Figure 8. C-scan comparison of bonded and unbonded, flat, fiber glass samples.

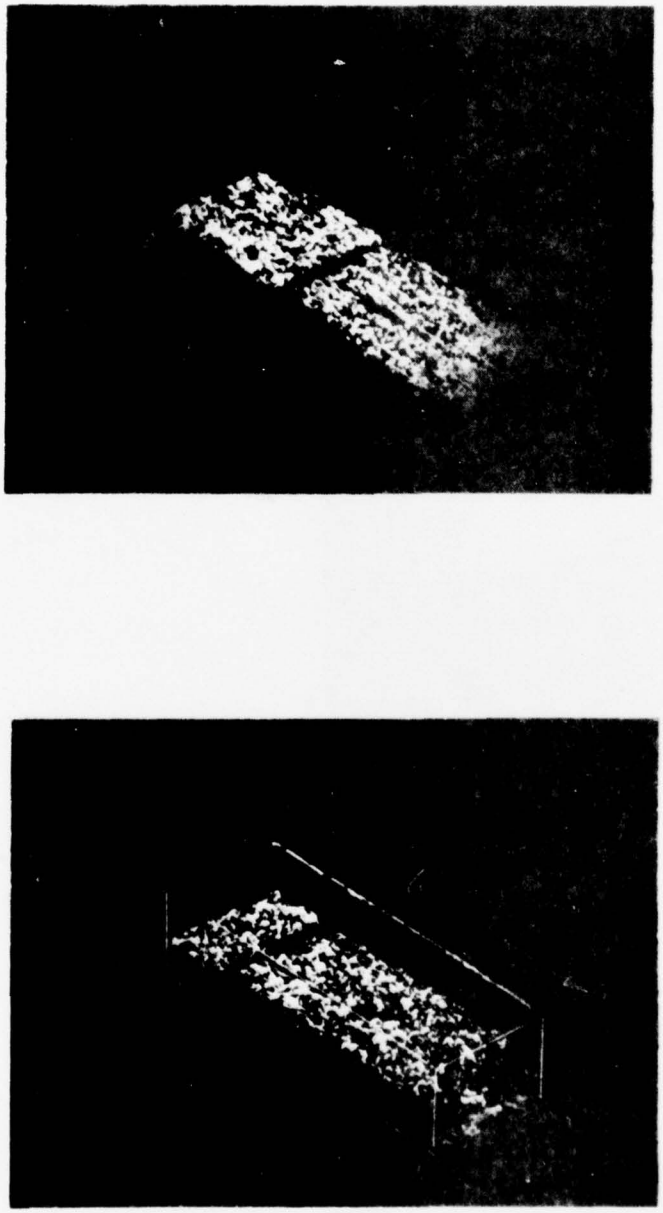

Figure 9. 3-D representation of the flat fiber glass sample.

C. Fiber Glass Cylinders

The objective of this test is to determine voids and/or debonding of composite cylindrical joints such as in the case of the 81MM XM73 Recoilless Rifle.

Figure 10 shows the cylindrical geometry of the two fiber glass test samples taken out of the 81MM recoilless rifle*. (Reference: Watervliet Arsenal Technical Report WVT-TR-74014: "Development of: Design Analyses, Manufacturing, and Testing of the 81MM XM73 Fiber Glass-Epoxy Recoilless Rifle", June 1974.) A pulse-echo method for disbond detection from the outer perifery of the fiber glass cylinders was employed. A metal liner was placed concentrically within each fiber glass cylinder. The assembly was mounted on a rotating fixture and immersed in the water below the scanner. Figure 11 shows the above setup. The signal reflected from the inner cylinder is detected by the gate. The absence of the gated signal would indicate the presence of a flaw.

Figure 12 show the geometry for this c-scan technique.

Figures 13A and 13B show the result of the c-scans for the bonded and unbonded cylinders. The large disbonded area can be clearly seen in Figure 13B. It is important to note the presence of numerous small disbonded areas in a section believed to have good bonding. This suggests that the frequency of occurrence of the disbonded areas may have to be correlated with their size to arrive at some acceptable inspection/rejection criterion.

*One cylinder had the scarf joint bonded. The second cylinder was held together through pressure (it was not bonded).

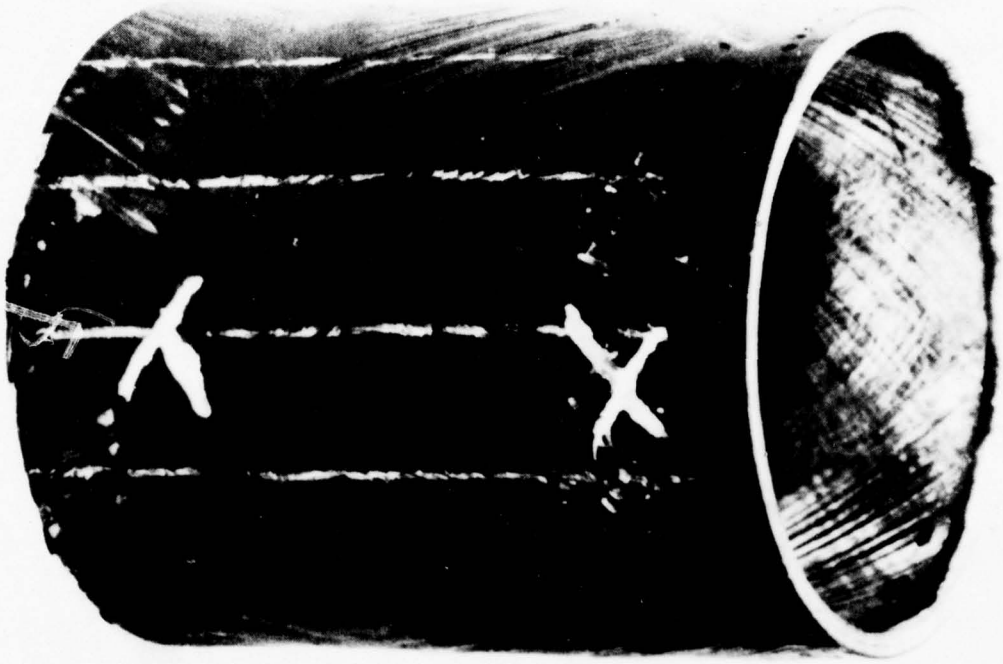

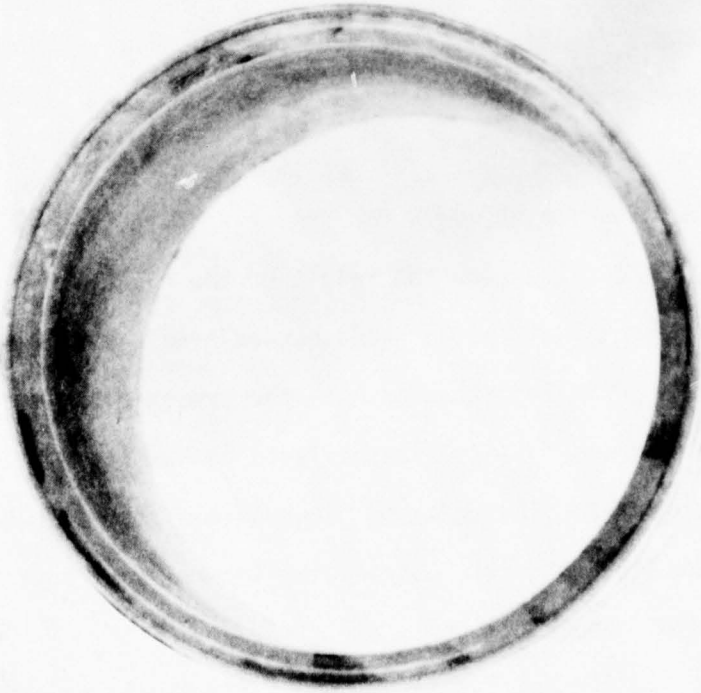

Figure 10. 81mm RCLR fiber glass epoxy chamber.

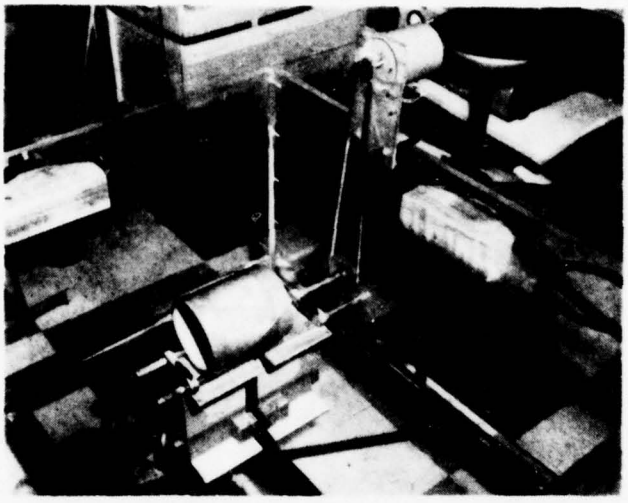

11A. FIBER GLASS CYLINDER ON ROTATING MOUNT

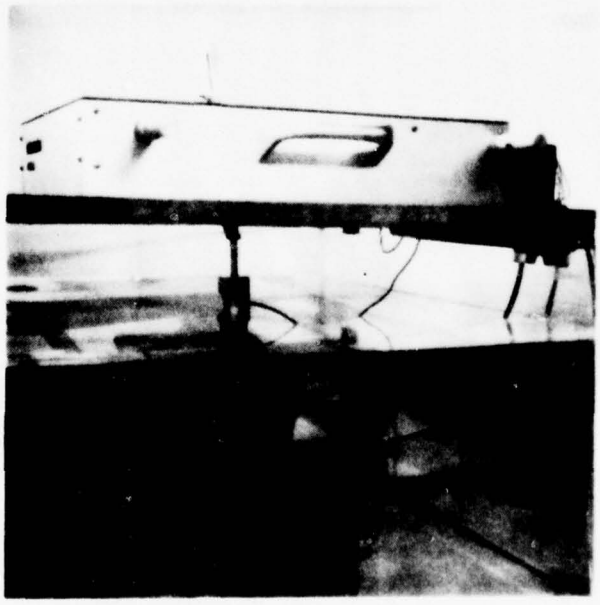

11B. ROTATING FIXTURE BELOW SCANNER

Figure 11. Fixture arrangement for inspection of fiber glass cylinders.

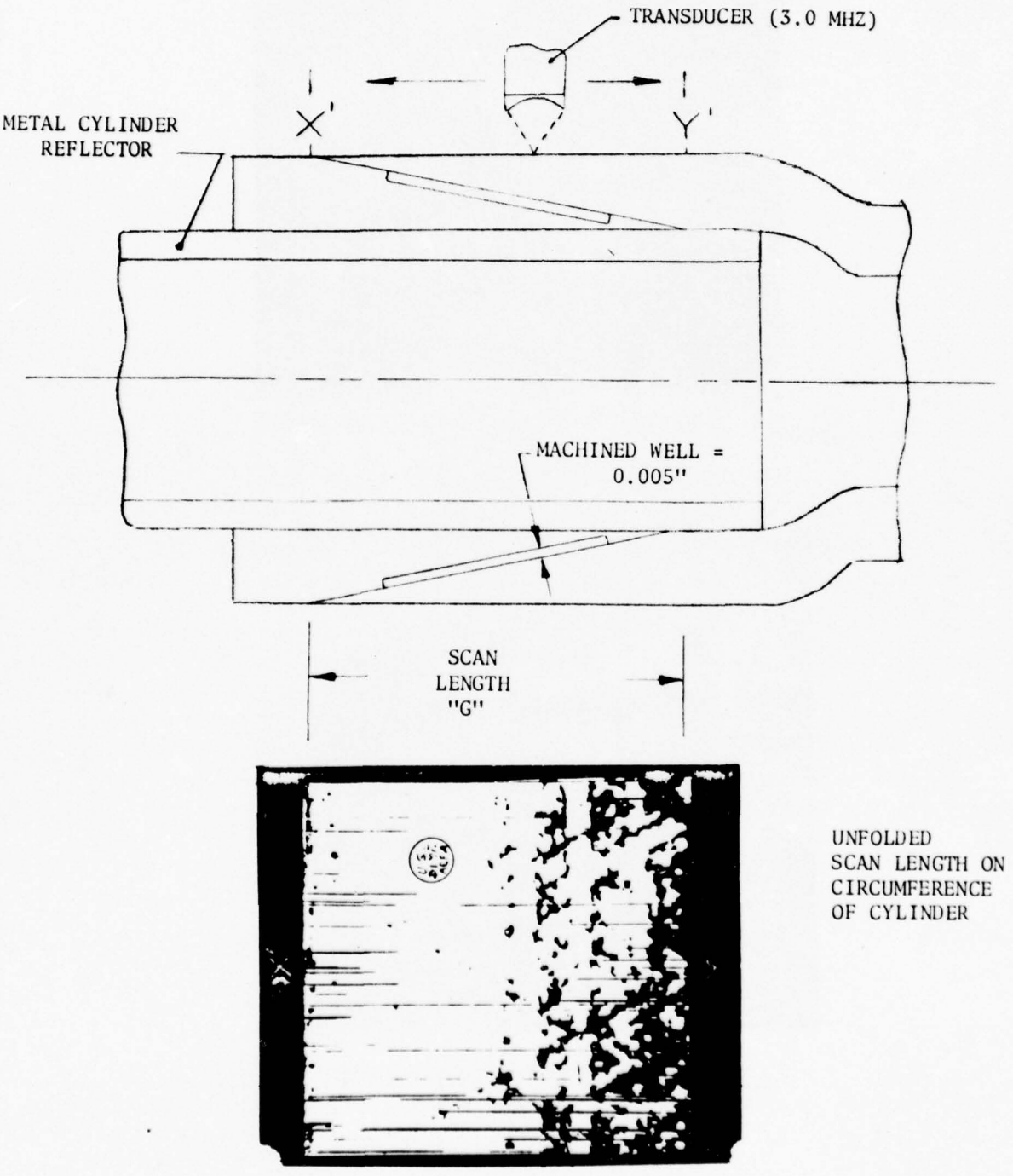

Figure 12. Test geometry and high line density C-scan disbond mapping.

13A. BONDED CYLINDER

13B. UNBONDED CYLINDER

Figure 13. Comparison of C-scans on bonded and unbonded fiber glass cylinders.

D. Standard Reference Fiber Glass Wound Cylinder

The objective of this test is to determine shape, size and location of voids in a fiber glass wound cylinder such as the 105MM M68 Thermal Shroud.

A composite fiber glass wound cylinder shown in Figure 14 was designed with flat bottom drill holes equally spaced midway around the cylinder for area size and depth distance comparisons. The first seven drill holes were all 1/4" deep and ranged from a diameter of 1/2" to 1/8" in steps of 1/16". The rest of the drill holes were 1/8" in diameter and varied in depth from 3/16" to 7/16" in steps of 1/16".

The test was conducted with the drill holes being at the bottom surface of the cylinder. The pulse-echo technique was used and a C-scan is shown in Figure 15A. The diameter size of the drill holes can be obtained using a 0.45x magnification from the original picture. Two of the drill holes have not been recorded due to the gate width that was selected in this run as demonstrated in Figure 15B. A B-scan of one half of the cylinder where the drill holes varied in depth is shown in Figure 16A. This is a side view projection of the planar defects as well as the top and bottom surfaces. Although the descending trend is clearly shown, a much better accuracy of the depth of each hole can be obtained if imaged alone with respect to the top and bottom surfaces as shown in Figure 16B.

Finally a 3-D projected image of approximately 1/3 of the cylinder is shown in Figure 17. In addition to the drill holes a number of other defects are observed in the material.

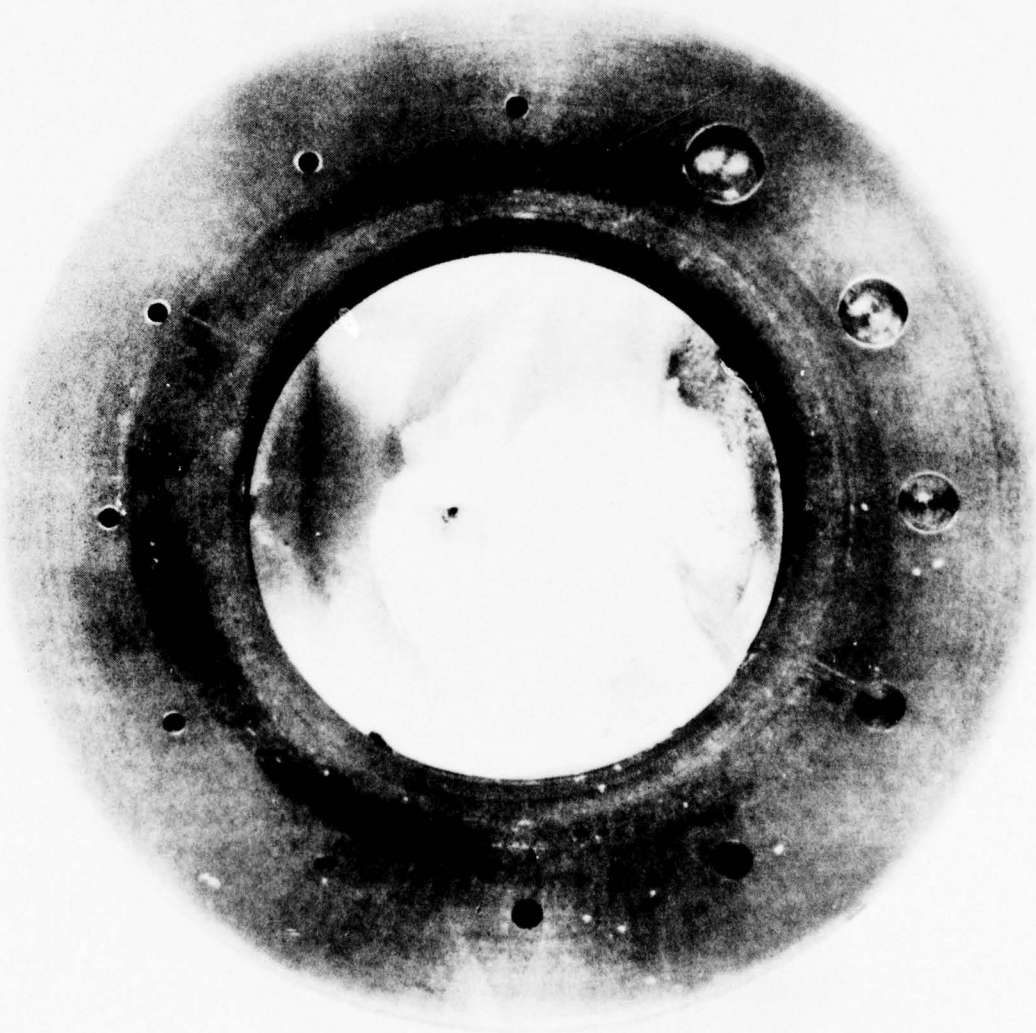

Figure 14. Standard reference fiber glass wound cylinder.

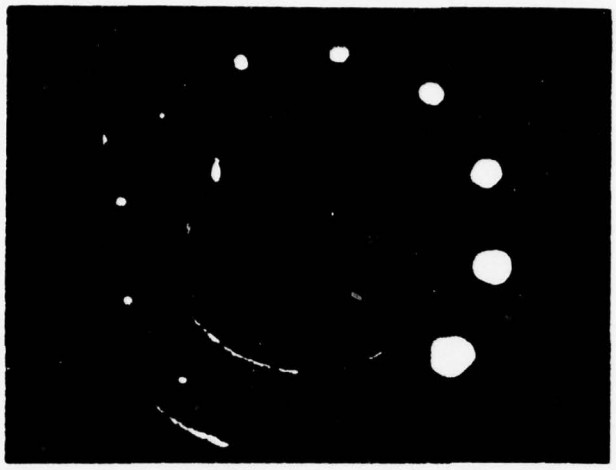

15A. C-SCAN SHOWING TOP OF ALL BUT TWO OF THE DRILL HOLES IN THE FIBER GLASS WOUND RING.

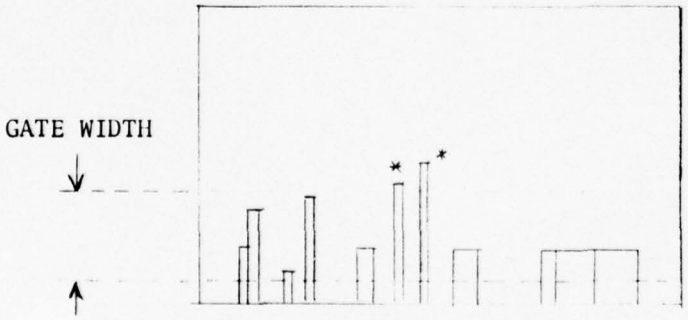

15B. SKETCH DEPICTING DRILLED HOLE ARRANGEMENT.

* NOTE: TWO OF THE DRILL HOLES ARE NOT SHOWN IN FIG 15A DUE TO THE SELECTED GATE WIDTH.

Figure 15. C-scan representation of fiber glass wound cylinder.

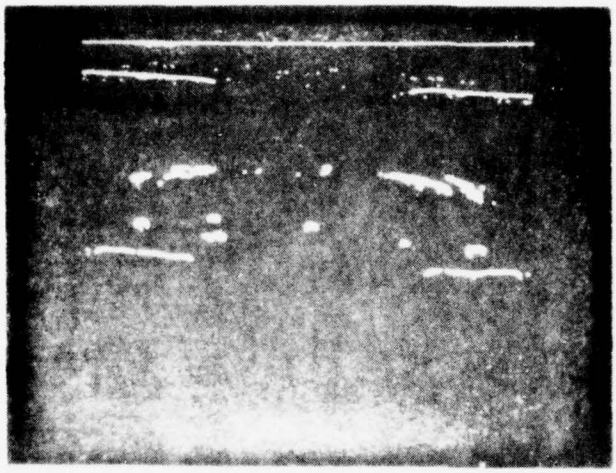

16A. B-SCAN OF THE DESCENDING DRILL HOLE ARRANGEMENT.

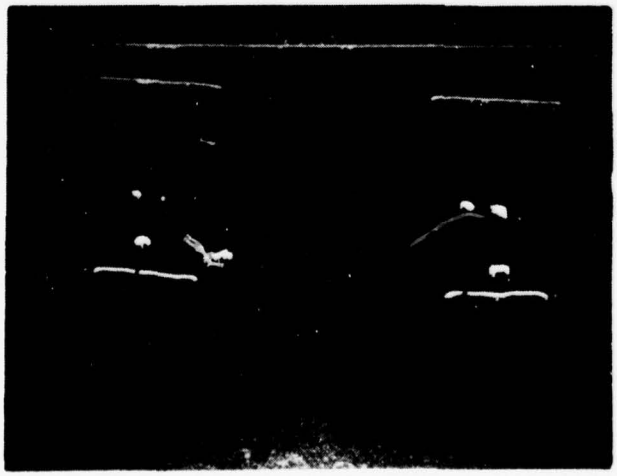

16B. B-SCAN OF SELECTED PLANAR DEFECTS (DRILLED HOLES).

Figure 16. B-scan representation of fiber glass wound cylinder.

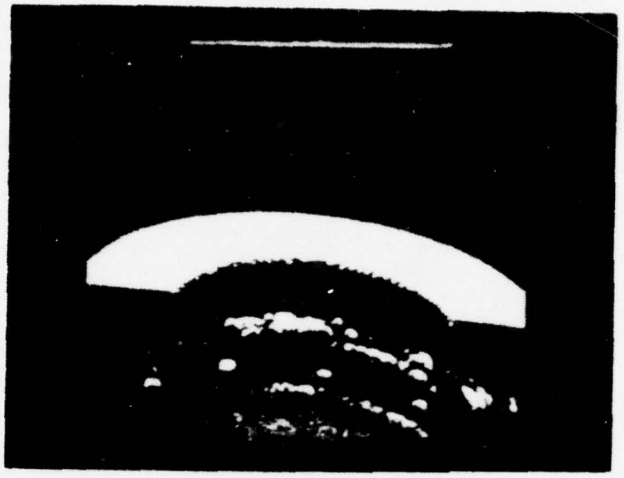

17A. 3-D PROJECTED VIEW

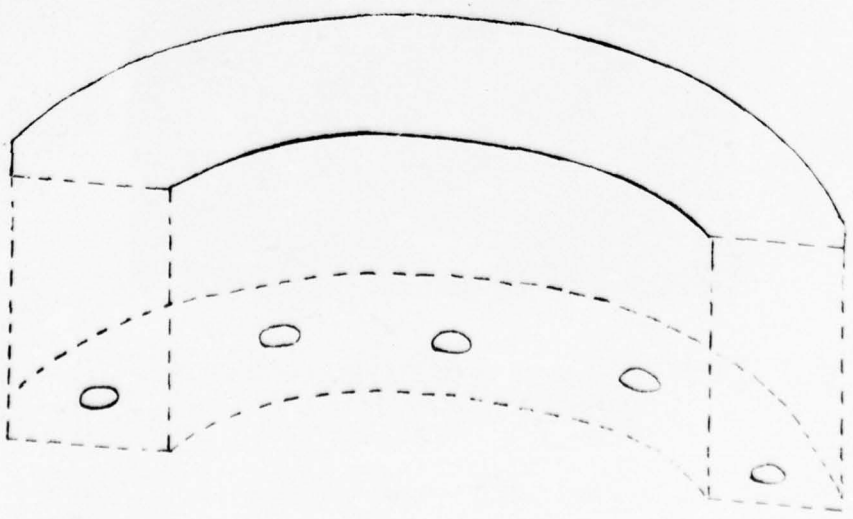

17B. SCHEMATIC DRAWING OF 3-D IMAGE

Figure 17. 3-D representation of fiber glass wound cylinder.

E. Gun Steel Fatigue Specimen

The objective of this test is to determine the shape, size and location of the crack induced in gun steel fatigue specimen. This information is presently used in determining fatigue life of the standard gun barrels.

A fatigue grown crack in a 4340 steel ASTM compact tension specimen is shown in Figure 18A. The importance of cracks in the fatigue life of structures has generated a considerable effort mainly in the accurate location of the crack depth. The approach adopted was to use a focused transducer and image the complete crack configuration as shown in Figure 18B. The results obtained show that the crack depth is not uniform throughout the sample and has a considerable lateral spread.

Figure 18C shows a C-scan of the same crack superimposed on a grid with a .036" step size. This approach provides a method for obtaining the complete depth information of the crack.

18A. ASTM COMPACT TENSION SPECIMEN

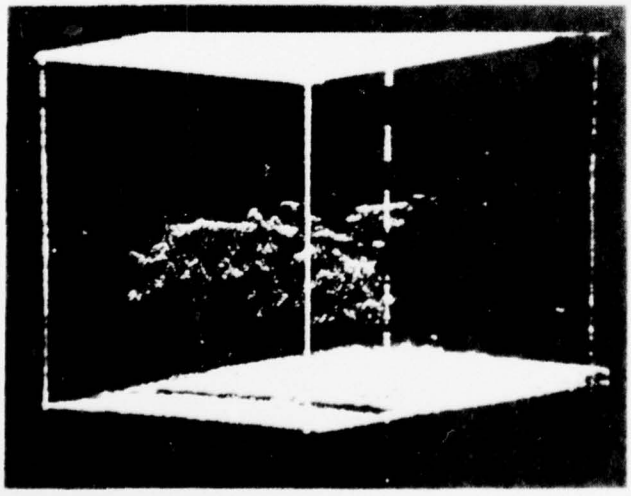

18B. 3-D VIEW OF CRACK CONFIGURATION

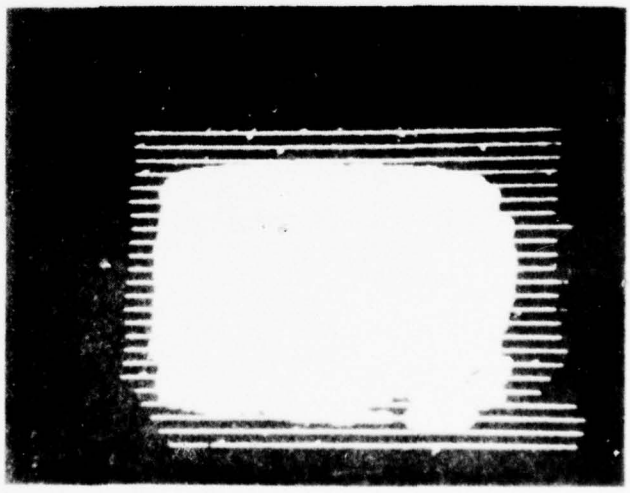

18C. C-SCAN OF CRACK SUPERIMPOSED ON 0.036" GRID

Figure 18. Gun steel fatigue sample.

F. Rotary Forge Billet

Of special interest to the rotary forging of gun tubes is the abiiity to inspect the interior structure of forged tubes. Figure 19A shows an arrangement for holographic inspecting a cylinder billet 15 inches in diameter and 15 inches long. Since in the original castings no flaws were detected two drill holes have been placed at the bottom of the cylinder. The holes are 3/8" in diameter and separated by a 5/8" spacing. The central hole is 3" long while its adjacent hole is 2 1/2" long. As observed in Figure 19B the central hole is in focus at the reconstructor's dial setting which corresponds to 12" away from the top surface. The adjacent hole is slightly out of focus because it is 12 1/2" away from the front surface. Figure 19C shows a print of the actual hologram used to reconstruct the object holes.

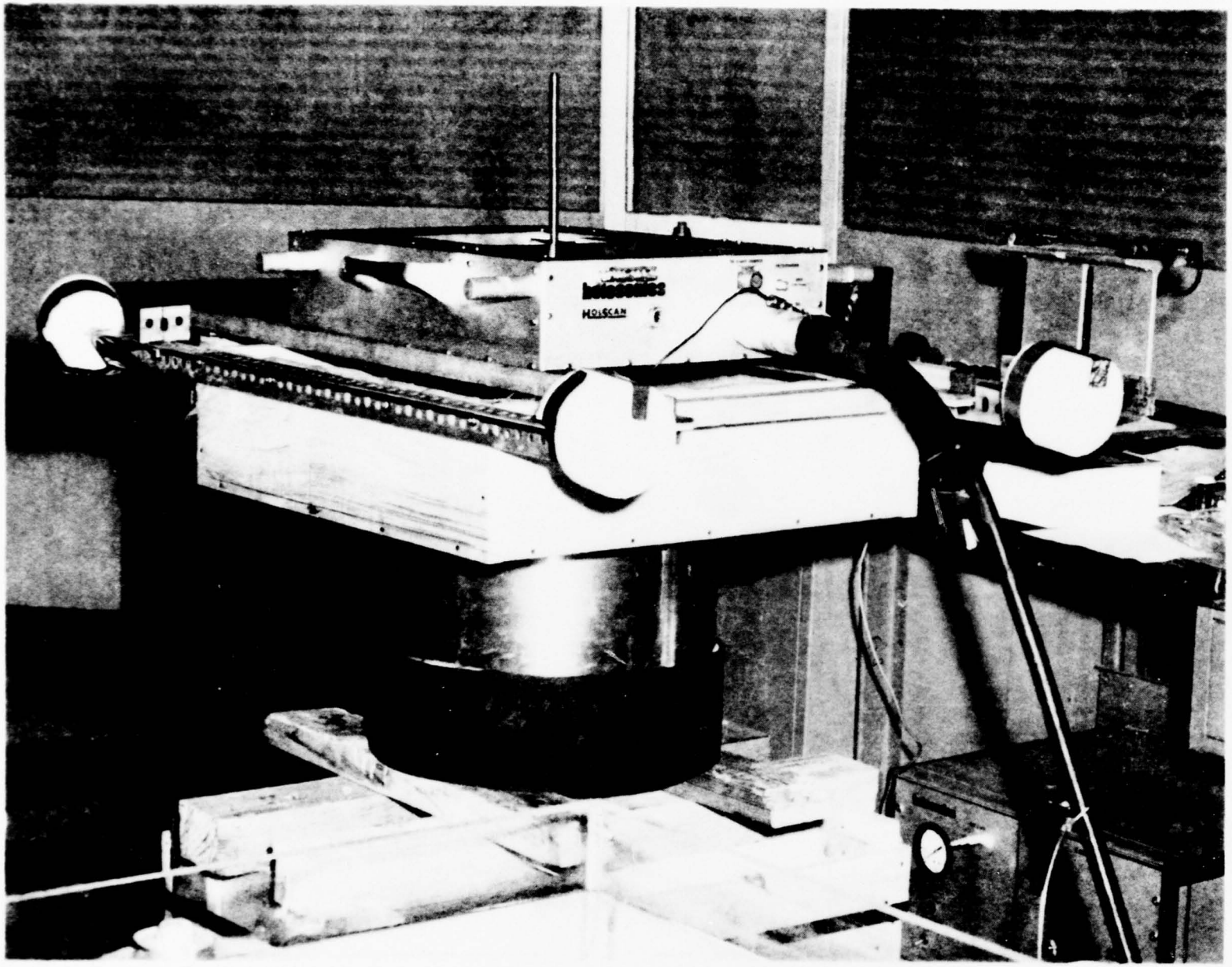

Figure 19A. Fixture for holographic inspection of rotary forge billet.

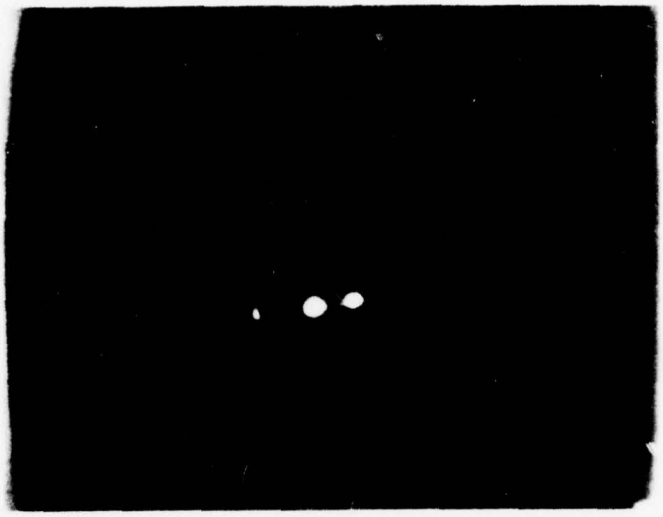

Figure 19B. Reconstructed image of planar holes through 12" of steel cylinder.

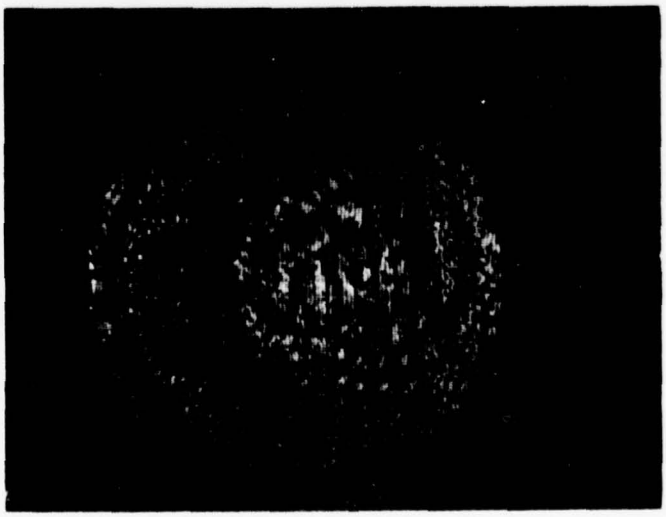

Figure 19C. 3 MHZ hologram of holes 12" deep in gun steel.

V. SUMMARY

The results reported in this study show that it is possible to inspect nondestructively many types of structures by means of either ultrasonic or acoustic holographic methods. The techniques described were demonstrated by determining delamination at the interface of composite joints as well as detecting and imaging voids that are present within the bonded composite regions. The use of steel test samples provided thick structures with flaw configurations that proved valuable in demonstrating some of the unique capabilities of the test methods employed. Through the use of standard reference samples and the selection of the proper test method the ability to image flaw size and shape within the interior of a solid structure with high resolution and sensitivity has been demonstrated.

Data presentation for each test method involved a visual recorded image graphically locating and displaying the flaw within the test structure. Also provided is accurate quantitative information on the location and structure of the flaw. As a result of these accomplishments in the field of ultrasonics and acoustic holography the design engineer may now selectively establish inspection criteria which will insure improved reliability and safety of military components such as the composite gun tubes and the recoilless gun launcher.

REFERENCES

1. B. B. Brenden and H. D. Collins, "Acoustical Holography with Scanned Hologram Systems", Holographic Nondestructive Testing, pp. 405-428, Academic Press, New York, 1974.
2. B. P. Hildebrand and H. D. Collins, "Evaluation of Acoustical Holography for the Inspection of Pressure Vessel Sections", Materials Research and Standards, Vol. 12, No. 12, p. 23, 1972.
3. H. D. Collins, "Acoustical Interferometry Using Electronically Simulated Variable Reference and Multiple Path Techniques", Acoustical Holography, Newell Booth, Editor, Vol. 6, Plenum Press, New York, p. 597, 1975.
4. D'Andrea, G. and Cullinan, R., "Application of Filament Winding to Cannon and Cannon Components. Part III: Summary Report", November 1976, WVT-TR-76035.
5. D'Andrea, G. and Cullinan, R., "Development of: Design Analysis, Manufacturing and Testing of the 81MM XM73 Fiber Glass-Epoxy Recoilless Rifle", June 1974, WVT-TR-74014.
6. D'Andrea, G. et al, "105MM Thermal Shroud", November 1972, WVT-7249.

APPENDICES

APPENDIX A

SYSTEM CALIBRATION *

* Technical information supplied by Holosonics for the optimum usage of the System 200

SYSTEM CALIBRATION

Plan View

Normal X/Y calibration is set such that a 6" x 6" aperture is presented as 4" x 4" on the storage monitor. X/Y calibration is accomplished by adjusting the X and Y gain pots in the storage monitor. This calibration is compatible with the optical processor (image reconstructor) calibration and should always be maintained when making acoustical holograms.

The calibration may be set for one to one image magnification for 'C' Scan of focused image holography.

Two switches on the X & Y circuit cards on the storage monitor allow the operator to select a 5X magnification of the standard X/Y calibration.

The image on Polaroid film from the C-5 camera will be .68 X the storage monitor calibration. If the storage monitor is calibrated to 4" x 4" for a 6" x 6" scanned aperture then the Polaroid image will be .45 x the scanned aperture.

The calibration on the storage monitor used with the 3-D module should be set so that a 6" x 6" scanned aperture is 4" x 4" on the storage monitor when the "tilt" and "rotation" controls are in their normal (plan view) position.

B-Scan or Z Axis Calibration

The .1 to 10 x depth magnification control is preset for a linear step function through its range of discrete steps. Two controls on the front panel of the 3-D module allow the operator to accurately adjust the basic calibration to compensate for the differences in velocities in various materials. A simple technique for accurate Z axis calibration is as follows.

1) Set the depth magnifica
2) Set the "rotation" control at normal
3) Set the "tilt" control at 90°

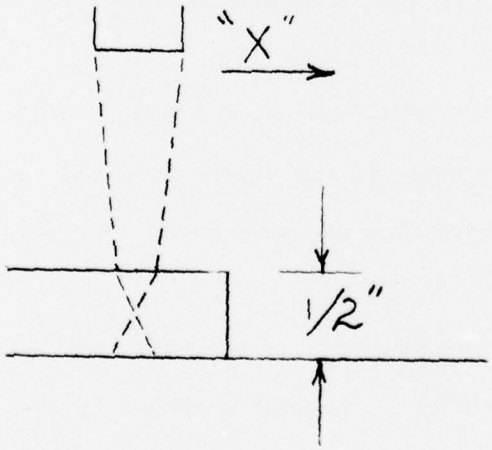

4) Set the scanner to scan on Zero increment a 3" scan at 1" per second in the "X" axis over a 1/2" thick aluminum block.
5) Set the gate to write the back surface of the aluminum block on the 3-D storage monitor.

6) With the "front surface" switch in the up position, the trace on the storage monitor should look like this.

7) Adjust the "couplant velocity" control to obtain the desired calibration for this 1/2" change in the water path.
8) Place the "front surface" switch in the down position.
9) Adjust the "material velocity" control to cause the back surface trace to fall in the proper plane. The section view of the 1/2" block should now look like this.

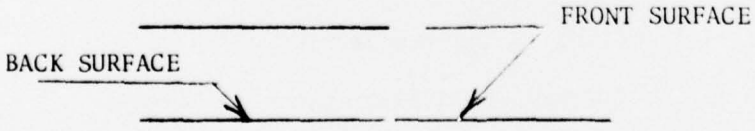

ACOUSTICAL HOLOGRAPHY EQUATIONS

1. $r_1 = r_m + (r_w - F)\frac{Vw}{Vm}$, when the focal point is at or above the metal surface.

where: $r_m = \frac{V_m t_m}{2} \times 10^{-3}$ (metal path in inches)

$r_w = \frac{V_m t_w}{2} \times 10^{-3}$ (water path in inches)

F = focal length in inches

V_m = velocity in metal in mils/μsec.

V_w = velocity in water in mils/μsec.

t = time in μsec.

r_1 = object distance from focal point in inches

2. $N = \frac{24.9f}{V_m}$

where: f = frequency in MHz.

V_m = velocity in metal in mils/μsec.

3. $S = \frac{9.6N}{r_1 - 0.696N}$

where: S = dial setting on the reconstructor.

r_1 = object distance from focal point in inches.

4. $M = 8.869\frac{N}{r_1}$

where: M = image magnification.

r_1 = object distance from focal point in inches.

EXAMPLE

TRANSDUCER
Frequency Used -
3.2MHz

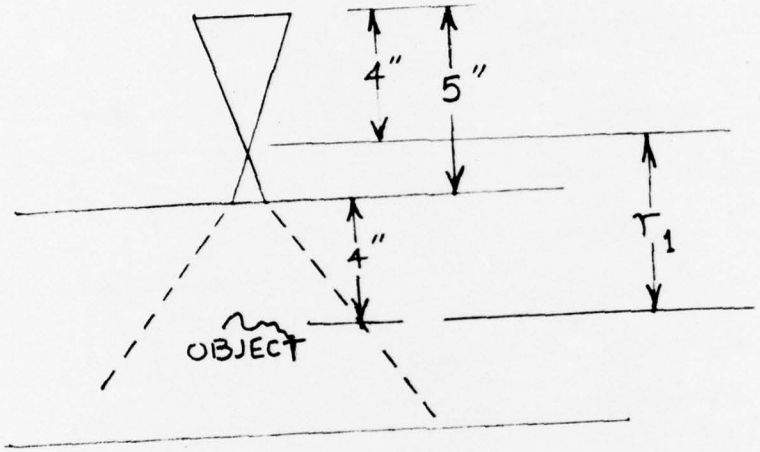

1. $r_1 = 4'' + (5'' - 4'') \frac{59.0}{250} = 4.236''$

2. $N = \frac{24.9(3.2)}{250} = .319$

3. $S = \frac{9.6(.319)}{4.236 - .696(.319)} = .763$

4. $M = \frac{8.869(.319)}{4.236} = .668$

LONGITUDINAL WAVE

ULTRASONIC IMAGING

TECHNIQUES

"A" SCAN PRESENTATION

r_w = water path

r_m = metal path

A = first surface

B = back surface

t_w = 16 μsec/inch in water

t_m = 4 μsec/inch in metal

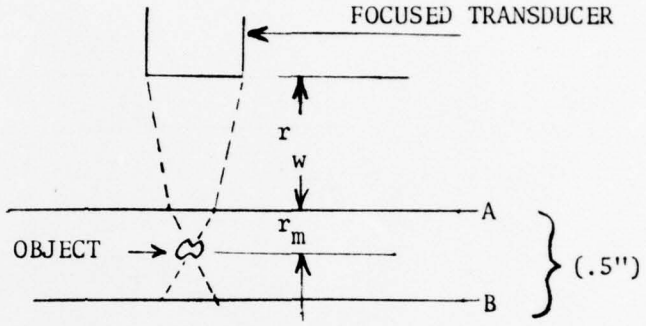

If r_w = .75 inches and r_m = .25 inches and the metal thickness is .5 inches, the "A" scan presentation on an oscilloscope would appear as shown below.

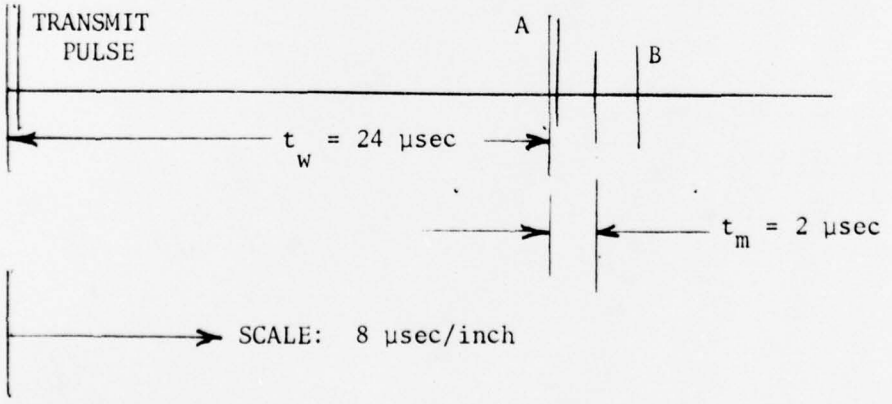

Note: Generally t_w must be > t_m. (In certain cases t_w may = 0)

"B" SCAN AND "C" SCAN TECHNIQUES

V_w = WATER VELOCITY = .062"/μsec.

V_m = METAL VELOCITY ≃.250"/μsec.

For "B" scan or "C" scan inspection, the best image resolution is obtained at the plane described by the focal point of the transducer in the test sample.

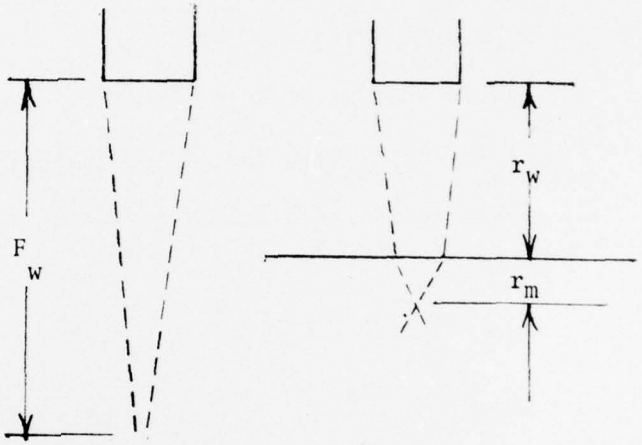

1) If F_w = 2 inches,

Then $F_m \simeq 1/2$ inch

Since

$F_m = F_w(\frac{V_w}{V_m})$ or $F_m \simeq \frac{F_w}{4}$

F_w = transducer focal length in water

F_m = transducer focal length in metal

2) Image resolution (ΔX) is a function of the active transducer diameter, the focal length in the material being inspected and the transducer frequency. (Resolution is not synonymous to sensitivity)

$\Delta X = 1.22\ \lambda_m(\frac{F_m}{d})$, WHERE d = active transducer diameter

Assume a 1/2" diameter X 2" focal length (F_w) transducer.

$\lambda_m = \frac{V_m}{f}$, f = frequency in MHz

THEN:

$$\Delta X \text{ @ } 3MHz = 1.22\ (\frac{.250}{3})\ (\frac{1/2}{1/2})$$

$$\Delta X \text{ @ } 3MHz = .102"$$

AND:

$$\Delta X \text{ @ } 5MHz = 1.22\ (\frac{.250}{5})\ (\frac{1/2}{1/2})$$

$$\Delta X \text{ @ } 5MHz = .061$$

3) The following formula is useful for positioning the focal point of the transducer at the desired depth in the test material.

$$r_w = \left(\frac{V_m}{V_w}\right)(-r_m) + F_w$$

Assume that we wish to place the transducer focal point at a depth of 1/2 inch below the top surface of the test piece and the transducer focal length is 4 inches in water,

THEN:

$$r_w = \left(\frac{250}{63}\right)(-1/2) + 4, \quad r_w = 1.98''$$

AND, $t_w = \dfrac{2r_w}{V_w} \qquad \therefore \quad t_w = 63.4\ \mu sec$

For most metals, the following approximation is sufficiently accurate.

$$r_w \simeq F_w - 4r_m$$

AND

$$t_w \simeq r_w\ (32)$$

OR FOR THE ABOVE CASE

$$r_w \simeq 4 - 4\ (1/2) \qquad \therefore \quad r_w \simeq 2''$$

AND

$$t_w \simeq r_w\ (32) \qquad \therefore \quad t_w \simeq 64\ \mu sec$$

GLOSSARY OF TERMS

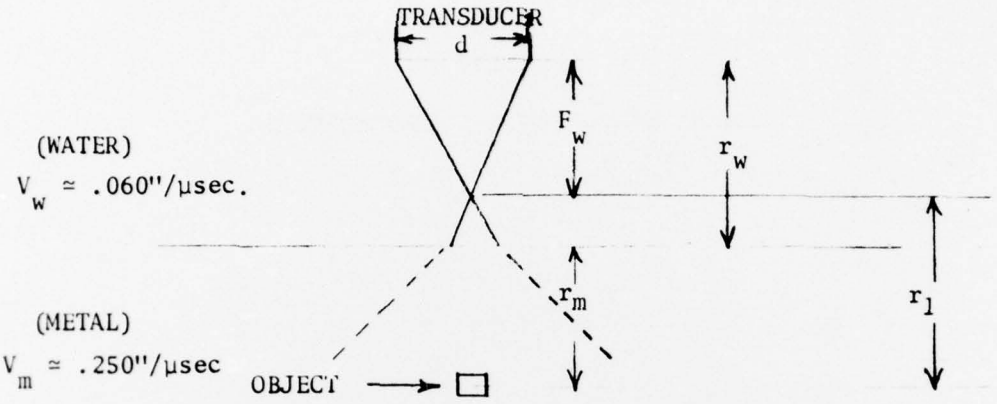

d = diameter of active transducer element

F_w = transducer focal length in water

r_w = water path in inches

r_m = metal path in inches

r_l = object distance from focal point in inches

V_w = velocity in water in mils/μsec

V_m = velocity in metal in mils/μsec

t = time in μ sec

f = frequency in MHz

M = image magnification

S = dial setting on reconstructor

N = light/sound wave length ratio

X = lateral image dimension

Δm = object distance tolerance

ΔX = lateral image resolution

F_m = transducer focal length in metal

t_w = ≃ 16 μsec/inch in water

t_m = ≃ 4 μsec/inch in metal

λ = wave length

APPENDIX B

81MM XM73 CHAMBER'S CONFIGURATION

81MM XM73 CHAMBER CONFIGURATION

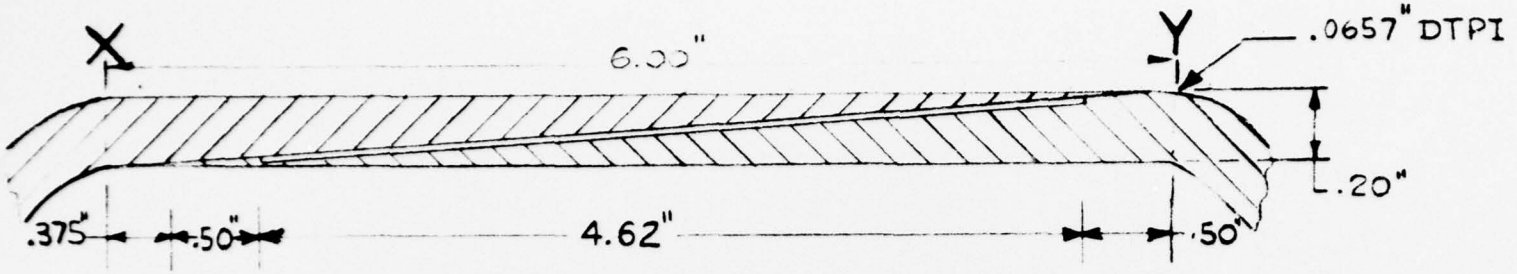

NOTE

1. Chambers tested have the same basic configuration shown in sketch.
2. Chamber depicted in Figure 10 is an adhesively bonded item which has been successfully test fired. In addition to what is shown in above sketch, the tube section has twelve (12) equally spaced bleeder slots going from the well to the Y location. These slots, which are ∿ 0.030" wide and 0.005" deep, allow excess adhesive to escape to the outside of the joint.
3. The C-Scan in Figure 13B depicts the nonbonded chamber in which the well was fabricated without the bleeder holes.
4. Both chambers have been marked internally (at x-end) to show location of the start of the well.
5. The X-Y notations shown on sketch and chambers, are reference locations.

WATERVLIET ARSENAL INTERNAL DISTRIBUTION LIST

May 1976

	No. of Copies
COMMANDER	1
DIRECTOR, BENET WEAPONS LABORATORY	1
DIRECTOR, DEVELOPMENT ENGINEERING DIRECTORATE	1
ATTN: RD-AT	1
RD-MR	1
RD-PE	1
RD-RM	1
RD-SE	1
RD-SP	1
DIRECTOR, ENGINEERING SUPPORT DIRECTORATE	1
DIRECTOR, RESEARCH DIRECTORATE	2
ATTN: RR-AM	1
RR-C	1
RR-ME	1
RR-PS	1
TECHNICAL LIBRARY	5
TECHNICAL PUBLICATIONS & EDITING BRANCH	2
DIRECTOR, OPERATIONS DIRECTORATE	1
DIRECTOR, PROCUREMENT DIRECTORATE	1
DIRECTOR, PRODUCT ASSURANCE DIRECTORATE	1
PATENT ADVISORS	1

EXTERNAL DISTRIBUTION LIST

December 1976

1 copy to each

OFC OF THE DIR. OF DEFENSE R&E
ATTN: ASST DIRECTOR MATERIALS
THE PENTAGON
WASHINGTON, D.C. 20315

CDR
US ARMY TANK-AUTMV COMD
ATTN: AMDTA-UL
AMSTA-RKM MAT LAB
WARREN, MICHIGAN 48090

CDR
PICATINNY ARSENAL
ATTN: SARPA-TS-S
SARPA-VP3 (PLASTICS
TECH EVAL CEN)
DOVER, NJ 07801

CDR
FRANKFORD ARSENAL
ATTN: SARFA
PHILADELPHIA, PA 19137

DIRECTOR
US ARMY BALLISTIC RSCH LABS
ATTN: AMXBR-LB
ABERDEEN PROVING GROUND
MARYLAND 21005

CDR
US ARMY RSCH OFC (DURHAM)
BOX CM, DUKE STATION
ATTN: RDRD-IPL
DURHAM, NC 27706

CDR
WEST POINT MIL ACADEMY
ATTN: CHMN, MECH ENGR DEPT
WEST POINT, NY 10996

CDR
HQ, US ARMY AVN SCH
ATTN: OFC OF THE LIBRARIAN
FT RUCKER, ALABAMA 36362

CDR
US ARMY ARMT COMD
ATTN: AMSAR-PPW-IR
AMSAR-RD
AMSAR-RDG
ROCK ISLAND, IL 61201

CDR
US ARMY ARMT COMD
FLD SVC DIV
ARMCOM ARMT SYS OFC
ATTN: AMSAR-ASF
ROCK ISLAND, IL 61201

CDR
US ARMY ELCT COMD
FT MONMOUTH, NJ 07703

CDR
REDSTONE ARSENAL
ATTN: AMSMI-RRS
AMSMI-RSM
ALABAMA 35809

CDR
ROCK ISLAND ARSENAL
ATTN: SARRI-RDD
ROCK ISLAND, IL 61202

CDR
US ARMY FGN SCIENCE & TECH CEN
ATTN: AMXST-SD
220 7TH STREET N.E.
CHARLOTTESVILLE, VA 22901

DIRECTOR
US ARMY PDN EQ. AGENCY
ATTN: AMXPE-MT
ROCK ISLAND, IL 61201

EXTERNAL DISTRIBUTION LIST (Cont)

1 copy to each

CDR
US NAVAL WPNS LAB
CHIEF, MAT SCIENCE DIV
ATTN: MR. D. MALYEVAC
DAHLGREN, VA 22448

DIRECTOR
NAVAL RSCH LAB
ATTN: DIR. MECH DIV
WASHINGTON, D.C. 20375

DIRECTOR
NAVAL RSCH LAB
CODE 26-27 (DOCU LIB.)
WASHINGTON, D.C. 20375

NASA SCIENTIFIC & TECH INFO FAC
PO BOX 8757, ATTN: ACQ BR
BALTIMORE/WASHINGTON INTL AIRPORT
MARYLAND 21240

DEFENSE METALS INFO CEN
BATTELLE INSTITUTE
505 KING AVE
COLUMBUS, OHIO 43201

MANUEL E. PRADO / G. STISSER
LAWRENCE LIVERMORE LAB
PO BOX 808
LIVERMORE, CA 94550

DR. ROBERT QUATTRONE
CHIEF, MAT BR
US ARMY R&S GROUP, EUR
BOX 65, FPO N.Y. 09510

2 copies to each

CDR
US ARMY MOB EQUIP RSCH & DEV COMD
ATTN: TECH DOCU CEN
FT BELVOIR, VA 22060

CDR
US ARMY MAT RSCH AGCY
ATTN: AMXMR - TECH INFO CEN
WATERTOWN, MASS 02172

CDR
WRIGHT-PATTERSON AFB
ATTN: AFML/MXA
OHIO 45433

CDR
REDSTONE ARSENAL
ATTN: DOCU & TECH INFO BR
ALABAMA 35809

12 copies

CDR
DEFENSE DOCU CEN
ATTN: DDC-TCA
CAMERON STATION
ALEXANDRIA, VA 22314

NOTE: PLEASE NOTIFY CDR, WATERVLIET ARSENAL, ATTN: SARWV-RT-TP, WATERVLIET, N.Y. 12189, IF ANY CHANGE IS REQUIRED TO THE ABOVE.